NASA SP-13

GEOPHYSICS AND ASTRONOMY IN SPACE EXPLORATION

NATIONAL AERONAUTICS AND SPACE ADMINISTRATION • Washington, D.C.
December 1962 • Office of Scientific and Technical Information

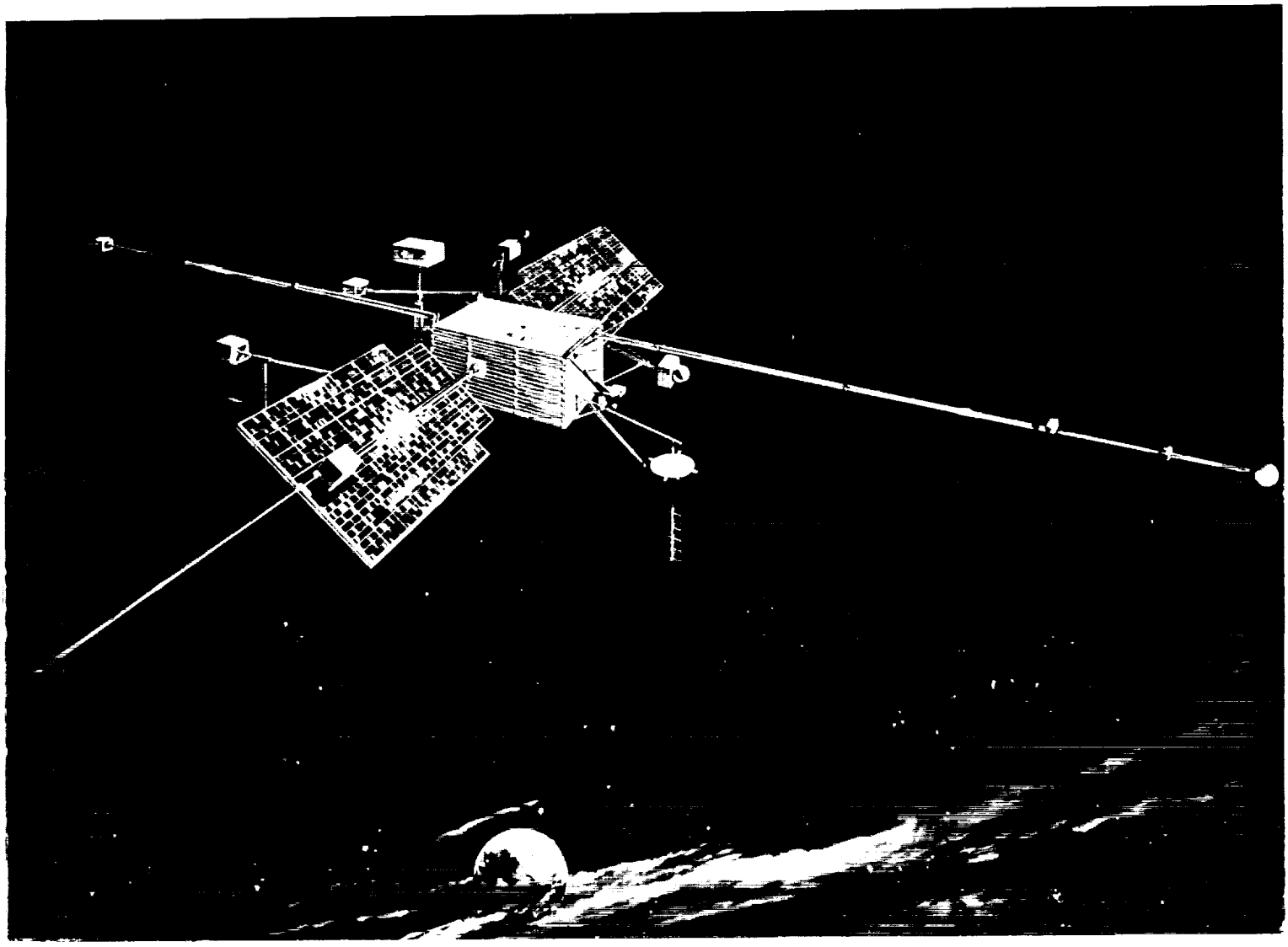

Foreword

The NASA-University Conference on the Science and Technology of Space Exploration, conducted in Chicago on November 1–3, 1962, was held "to provide an authoritative and up-to-date review of aeronautical and space science technology."

The scientific papers delivered at the conference were grouped for presentation by topics and are, in effect, 1962 state-of-the-art summaries. Accordingly, NASA has published under separate covers sixteen groups of conference papers to make them conveniently available to those interested in specific fields. This series (NASA SP–13 to NASA SP–28) is listed by title and price on the back cover.

All papers presented at the conference have also been published in a two-volume *Proceedings* (NASA SP–11) available from the Superintendent of Documents for $2.50 and $3.00, respectively. Those papers presented herein originally appeared on pages 107 to 151 of Volume 1 of NASA SP–11.

For sale by the Superintendent of Documents, U.S. Government Printing Office
Washington 25, D.C. - Price 35 cents

Contents

Sounding Rocket as a Tool for College and University Research

By Eleanor C. Pressly

MISS ELEANOR C. PRESSLY *is Head of the Vehicle Section, Sounding Rockets Branch of NASA's Goddard Space Flight Center. She has been with Goddard virtually since its inception and now has an important part in conducting NASA's sounding rocket program. She holds an A.B. degree from Erskine College, and an M.A. degree from Duke University. A former mathematics teacher, she became a mathematician at the Radio Research Laboratory at Harvard University. In 1945 she joined the Naval Research Laboratory as a mathematician and later became an aeronautical research engineer in the Rocket Sonde Branch. She has been closely associated with the Navy's Aerobee-Hi rocket and has followed the development of this vehicle to its present configuration, now in use by NASA. Miss Pressly is a member of the American Rocket Society.*

The sounding rocket is, indeed, an extremely useful tool for research in the space sciences. Since the end of World War II, it has provided the means of obtaining information about our upper atmosphere that up to that time had been unattainable. Under the NASA sounding rocket program, it is used by colleges and universities for scientific investigations in the various disciplines of geophysics and astronomy. The program now includes more than 10 schools in this country who are already conducting experiments and there are some cooperative projects with foreign countries. I hope to show the advantages of the sounding rocket and the method by which a college or university may participate in such research. Let us look at a few examples of what is being accomplished in the NASA program. These particular experiments have been chosen in order to represent different rocket techniques.

In the ionospheric research program, which was discussed in the Geophysics and Astronomy session yesterday, there was a series of three flights to measure electron temperature and charge density as a function of altitude using the Langmuir probe and the R.F. Resonance Probe techniques. Thus there were two independent means of taking the same measurements simultaneously. Two of the flights were made at midday and one at night in order to study the temporal changes. Data were collected between 95 and 125 kilometers on each flight. An artist's conception of the payload is shown in figure 10–1. The forward payload housing was of a clam shell design which was ejected before the data collection altitude. This opened up

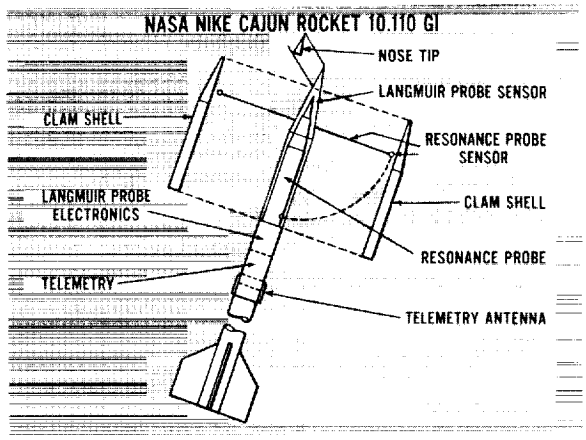

FIGURE 10–1.—D-region ionosphere experiment.

the Langmuir Probe sensor, which was mounted inside the nose tip, and permitted the R.F. resonance probe antennas to be erected. All three flights were successful, and immediate post-flight results confirmed agreement between the two techniques. On the night flight both instruments recorded a sporadic layer 3 kilometers thick, beginning at 102 kilometers on both up and down legs of the trajectory.

Yesterday morning the Particles and Fields program was discussed. Two projects in that program are mentioned below.

During the fall of 1960 a series of 14 rockets was flown from Fort Churchill, Manitoba, Canada, to study the beams of high energy nucleons, which balloon experiments had shown to arrive at the earth following many large solar flares. Both nuclear emulsions and counters were used, and recovery was required for the emulsions. These experiments were prepared and held in a standby condition awaiting solar activity. Nine flights were made during the solar flare period 11 to 18 November. Figure 10–2 shows some of the results obtained from an emulsion flown on November 12. In all, ten of the nuclear emulsion packages were recovered and all except one of the flights produced good telemetered data. This project was increased after the field operation began, and it was accomplished with only nine payloads. The payloads that were recovered can be flown again if the need arises.

Another series of three experiments was made to determine the altitude and intensity of electric current systems over Wallops Island, Virginia, using a proton precession magnetometer. Care was taken to make the rockets as nonconducting as possible, a special fiber glass payload housing having been designed especially for this experiment. The 50 pound payloads were carried to 200 kilometers altitude. On one of the flights, which took place during a magnetic storm, electric currents were found at 130 kilometers altitude. On another, fired during a magnetically quiet period, no currents were found over Wallops Island. One of the purposes of these flights was to prove out an instrument to be used in investigation of the equatorial electrojet. This follow-on project is now underway and will be carried out from a firing base in India during the spring and summer of 1963. Usually the experimenter wants his payload to maintain a stable, erect attitude; in this case the experimenter complained because two of the rockets remained so stable as to make his data reduction difficult.

In the aeronomy and D-region ionosphere disciplines both of which were subjects of previous discussion during this conference there are several synoptic experiments that are continuing programs. Atmospheric winds and diffusion are measured in the region of 60 to 190 kilometers by the sodium vapor release technique, with data being recorded by triangulation photography. Figure 10–3 is a photograph of the sodium cloud as seen at one camera site. The sodium experiment has stimulated the interest of scientists of a number of countries, and during the period of November 26 through December 13 of this year the first series of international

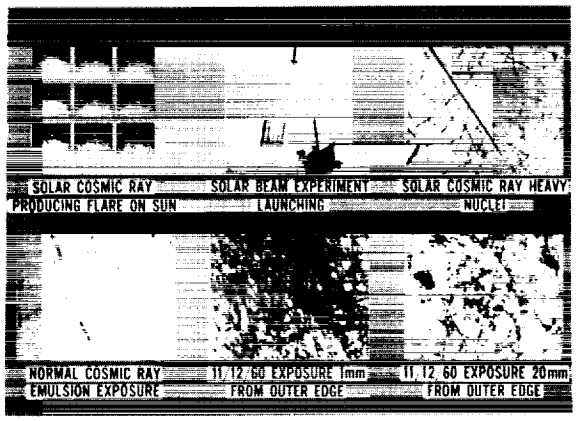

FIGURE 10–2.—Solar cosmic ray experiment.

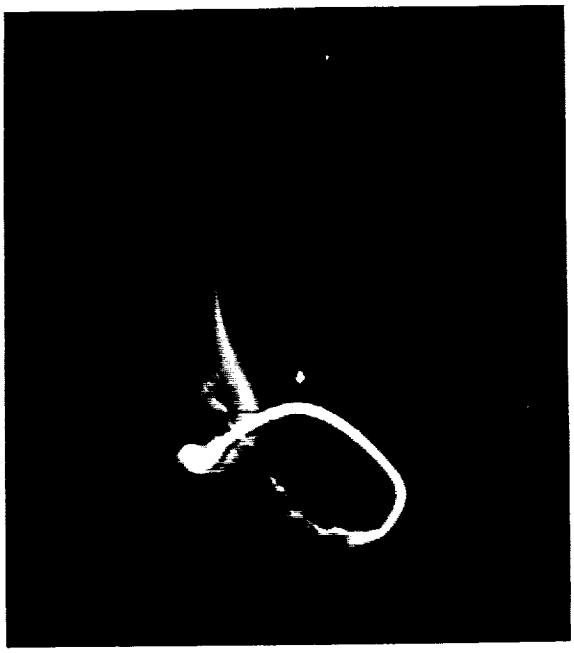

FIGURE 10–3.—Sodium vapor cloud.

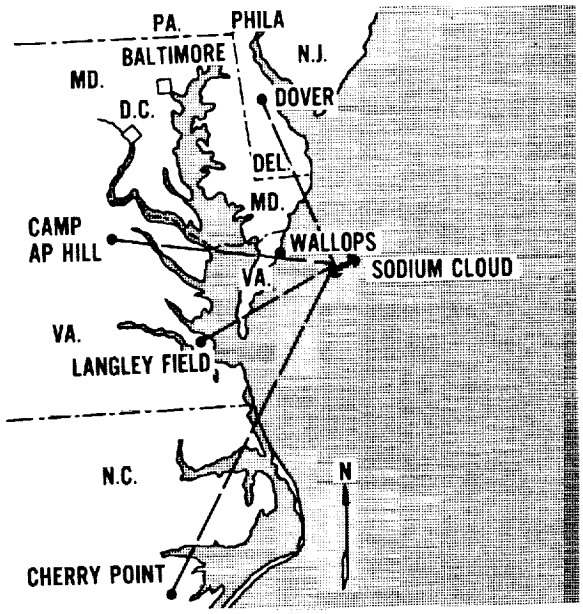

FIGURE 10–4.—Camera site locations for sodium vapor tests.

firings will be undertaken. Camera stations record the cloud produced by released sodium vapor. As shown in figure 10–4, the cameras are located on the ground along a circle of radius of the order of 100 kilometers from the firing site. These firings are made at twilight or dawn, when the sodium trail is sunlit but the scattered sunlight is low.

A companion to the sodium experiment is one that measures winds and temperatures between 25 and 90 kilometers by ejecting and exploding grenades during rocket ascent. Figure 10–5 is representative of what takes place. The time and direction of the sound arrivals are recorded by an array of sensitive microphones on the ground. From these data, winds and temperatures are determined in the altitude layer between each pair of grenades.

A third synoptic experiment is the measurement of electron density and electron temperature in the ionosphere. Figure 10–6 shows this type of payload. It is representative of the payload packaging technique one uses in research with rockets.

NASA will fly these three experiments as coordinated launches from Wallops Island and Fort Churchill. Wind data obtained by the grenade method and the sodium method will be compared. The ionosphere experiment will use these wind data for comparison with the electron density profile to look for a possible correlation between the strong wind shears observed and sporadic E. Other experiments in this synoptic program measure atmosphereic structure and composition.

Several groups are preparing rocket astronomy payloads designed for spectroscopy and stellar and nebular photometry. These were presented yesterday morning. Such payloads are relatively heavy (about 200 pounds) and peak altitude is on the order of 200 kilometers.

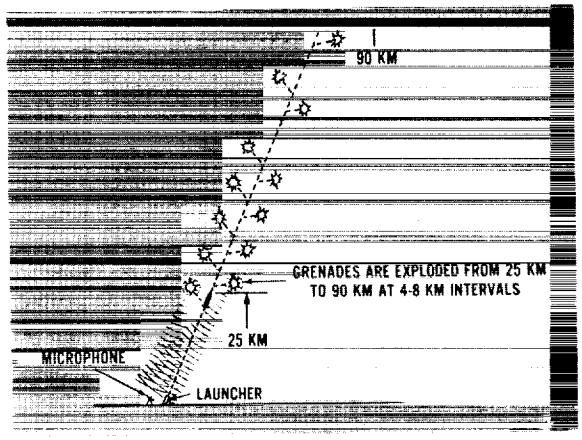

FIGURE 10–5.—Grenade test.

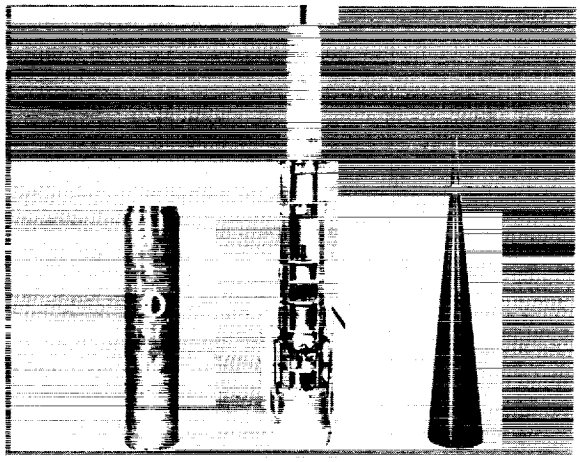

FIGURE 10–6.—Payload for electron density measurement in the ionosphere.

An altitude control system has been developed primarily for these experiments. An artist's sketch appears in figure 10–7. This system is capable of pointing the entire vehicle to a star with an accuracy of $\pm 2°$ and holding that position to within $\pm 1/4°$. It can, for example, point to as many as five different distinct targets in one flight with approximately 50 seconds of observing time at each position. A fine altitude control system is under development; it is to have a pointing accuracy of $\pm 30''$. These flights will also be testing the performance of various components, both mechanical and electrical, that are to be used in the Orbiting Astronomical Observatory.

In another experiment a mass spectrometer was carried to 960 kilometers to detect the presence and possibly the relative abundance of helium and hydrogen ions and to measure electron temperature and ion density.

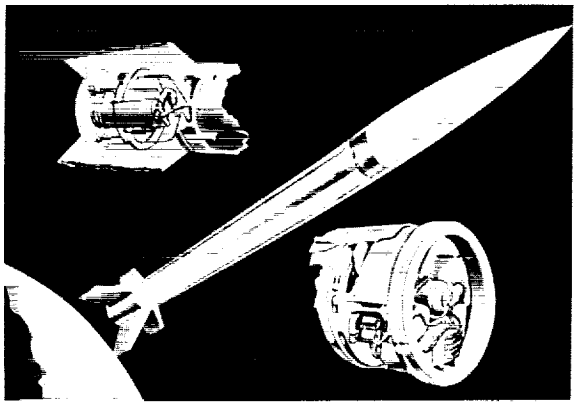

FIGURE 10–7.—Aerobee for rocket astronomy.

The highest altitude sounding rocket flight to date carried a radio astronomy experiment to measure the intensity of radio frequency energy that originates in the halo of our galaxy. The payload reached 1700 kilometers and had a data collection time of more than 20 minutes. The sensing system included a 40 foot tip-to-tip electric dipole deployed from the payload compartment after nose cone separation. The three radiometers operated simultaneously from the dipole antenna. From all indications this flight was a complete success.

There are many questions in all of the scientific disciplines that have not been answered. New groups are encouraged to participate in these investigations. NASA Headquarters will be receptive to proposals for experiments to be flown on sounding rockets. There are groups within NASA who are equipped to give guidance in all areas that may be new. Also, NASA is prepared to supply all support instrumentation—that is, telemetry, power supply, performance gages, aspect gages, calibrator, commutator, and all rocket wiring external to the experiment package. NASA can supply mechanical hardware such as payload racks, nose cone ejection systems, and special windows and antenna mounts. In other words, the experimenter is responsible for his own scientific instrumentation, and everything else is provided as government-furnished equipment. Some experimenters prefer to build the entire payload package. In this event NASA can provide consultation and advice.

NASA makes available all vehicles, performance analyses, and project coordination. Included with the vehicles are standard nose cones, payload housing extensions and, for certain of our vehicles, such accessory equipments as an attitude control system, recovery packages, special types of nose cones, and de-spin systems. The particular characteristics and the predicted performance data of all of the rocket systems are available. Special performance calculations and heating and stress analyses are made on an individual case basis as required. Contact is maintained between the scientific experimenter and others who are providing support during

the payload buildup period, and arrangements at the firing range are made.

NASA's family of rockets at the present time includes seven vehicle systems. Figure 10–8 is representative of these vehicles. An attempt has been made to arrive at a group with payload-altitude capabilities suited to experimenters needs, and the same model is fired over and over again for reliability. These seven systems cover the altitude regime between 100

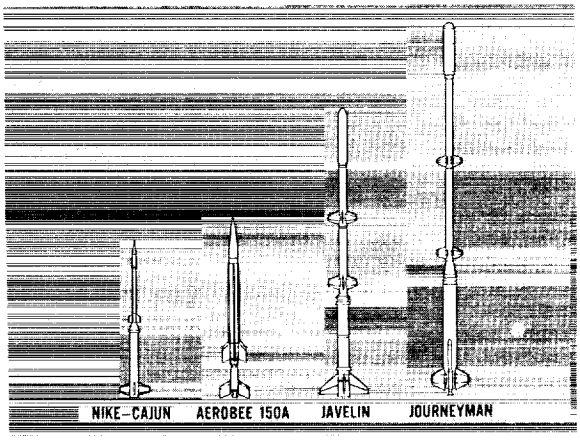

FIGURE 10–8.—Family of sounding rockets.

and 2500 kilometers. Figure 10–9 shows the performance capability of each of these vehicles. Calculations are for sea level launch at the standard firing elevation angle for each rocket. Net payload is defined as all additions to the basic vehicle, and it does not include the standard nose cone housing. Recovery systems have been developed for the Nike Cajun, Nike Apache, Aerobee 150A, and Journeyman. As the need for other capability arises and as proven vehicles become available to meet that need, such vehicles will be added. Most of these vehicles have been used in several different scientific disciplines.

The weight and volume characteristics of payloads that can be flown on rockets available to us now are shown in figure 10–10. Notice that except for the 500–700 kilometer region, the range to 2500 km is relatively well covered by some payloads.

The time required to prepare a payload for firing varies with the specific experiment and the amount of NASA support equipment neces-

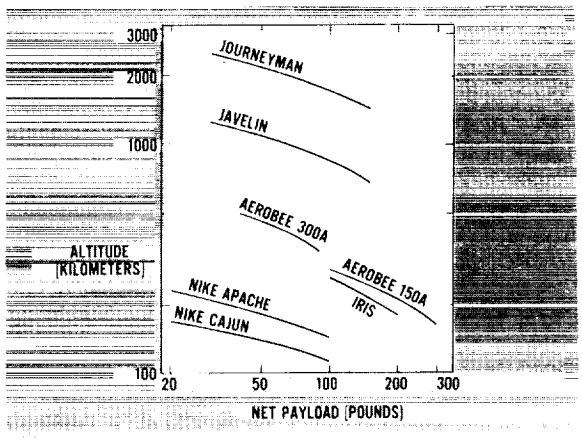

FIGURE 10–9.—Sounding rocket peak altitude in terms of payloads.

sary. The minimum time period is about six weeks, but such timing presupposes that the experimenter will be responsible for the whole payload package and that rocket vehicles and time on the firing range are available. Formal notification to all firing ranges is required at least 30 days before the expected launch date. A more normal and comfortable time interval is six months; and for large projects geared to specific time periods, such as the International Quiet Solar Year, planning a year or so in advance is appropriate.

NASA's primary firing site for sounding rockets is Wallops Island, Virginia. All of the vehicles may be fired from that range. Other ranges from which NASA may launch certain vehicles are: Fort Churchill, White Sands Missile Range, Pacific Missile Range, and Atlantic Missile Range. In addition through inter-government agreements, ranges are being or have

NET PAYLOAD RANGE WEIGHT (POUNDS)	MAXIMUM DIAMETER (INCHES)	MAXIMUM USEFUL VOLUME (CUBIC FEET)	ALTITUDE RANGE (KILOMETERS)
20 – 100	6.5	1	230 – 110
100 – 200	12	4.8	260 – 180
100 – 300	15	10.8	280 – 160
40 – 90	8	0.9	500 – 340
30 – 150	18.25	3.7	1250 – 680
30 – 150	18.25	4.9	2500 – 1400

FIGURE 10–10.—Sounding rocket payload statistics.

672058 O–63—2

been set up in India, Norway, Sweden, and Italy. At the present time these latter ranges can accommodate the Nike boosted vehicles only.

Let us look at the procedure one uses to obtain NASA approval to do research by means of sounding rockets.

If you are interested and have an experiment you would like to conduct, you should discuss it with NASA representatives who are working in the same scientific discipline as your experiment. They will probably suggest that you talk with the rocket support group at Goddard Space Flight Center as to the support available. You will be asked to prepare a proposal for presentation to NASA Headquarters. Your proposal should include what you hope to accomplish by your experiment, the method by which you obtain your data, the time period you will require, and the number of firings you wish to make. It should also include a statement of the support you will need from NASA. It is not necessary that you specify a particular rocket type; however, you will probably have determined the best rocket vehicle. Your proposal will be reviewed for its scientific value and for our ability to provide the support you require.

After your project receives approval and the funding arrangements have been made, we are in a position to make detailed plans. A conference that includes all groups who will be providing support to the operation is arranged. The areas where support is needed are determined, and a time schedule is set up. The result of this conference is that each group will know their responsibility and what they may expect from each other group. A complete interference check of the entire payload is required at Goddard before the payload is taken to the firing site. During this period environmental tests will be conducted and the payload dynamically balanced if these are considered necessary. The payload is mated to the rocket at the firing site. Preparation time there varies, depending on the number and complexity of the various tests that must be run. When the rocket has been fired, all telemetry and tracking records are provided to the experimenter.

There are many reasons why we use the sounding rocket both as a complement to and preparation for satellite experiments. It provides a vertical cross section of the atmosphere, and it reaches altitudes between balloon peak altitude and satellite perigee. It can be flown from selected places and at selected times; thus special events can be covered. Preparation time is short and the program is sufficiently flexible that discoveries can be followed up quickly. An experiment can be flown many times on a sounding rocket to once in a satellite. This enables the scientist to modify his experiment after a few firings and so broadens the total amount of information obtained. Similarly it is good for synoptic work in which the same experiment is repeated over a period of time. Usually one experimental group instruments the whole scientific payload and can use the entire flight time to best advantage, thus avoiding problems of compatibility between experiments. The sounding rocket is relatively inexpensive, and the logistics of firing it are relatively simple.

A considerable number of sounding rockets have been used as proving grounds for satellite experiments. Since one is doing basic research, it is appropriate to use the sounding rocket as a means of determining the best experimental approach to the satellite experiment, the areas of greatest interest, and the proper gains to set so that all data return from the satellite will be meaningful.

Most of these advantages of the sounding rocket contribute to making this program a good training for those who are beginning to do research using rockets and satellites.

During the several years since the beginning of NASA, 191 sounding rockets have been flown. Of these, 20—or 10%—have been college or university prime experiments. Another 31 flights, 16% of the total, have had college or university support. During 1962 there have been 18 flights in which colleges and universities participated, and 17 are planned for the rest of the year. If these flights are all made, the college and university participation will be 43% of the total program during 1962.

Space Flight Studies of the Ionosphere

By Robert E. Bourdeau

ROBERT E. BOURDEAU *is Head of the Planetary Ionospheres Branch at the NASA Goddard Space Flight Center. In addition to these duties, he was Project Manager for Explorer VIII and Project Scientist for the first international satellite, Ariel, and for S-66, the ionosphere beacon satellite. Mr. Bourdeau was formerly with the Naval Research Laboratory, assisting in upper atmosphere research with the V2, Aerobee, and Viking rockets, and later in atmospheric electricity research using aircraft. He received the B.S. degree in physics in 1943 from the University of Massachusetts, and is a member of the American Geophysical Union.*

SUMMARY

Results from rocket and satellite experiments designated to study the characteristics of charged particles with thermal energies which comprise the ionosphere are discussed. Data obtained since 1959 are compared with ground-based observations and with spaceflight data on the ionizing flux. This comparison then is used to update models of the ionospheric D, E, and F regions. In addition, model concepts of the upper ionosphere up to 2000 km including the helium ion layer and the lower protonosphere are presented. The research areas needing the greatest attention are outlined.

INTRODUCTION

Ionospheric physics is the study of the characteristics of charged particles with thermal energies, a group which exerts the greatest influence on the propagation of radio waves. The study necessarily includes the causal relationships between the charged particle characteristics, the ionizing sources, and the ionizable constituents.

Previous to spaceflight, knowledge regarding upper atmosphere ionization was obtained from ionosondes, which are radar-like methods based upon the reflection of radio waves by the ionized regions. Early observers using this technique were convinced that the daytime ionization was concentrated in three separate and distinct layers which they called E, F1, and F2. This incorrect conclusion was primarily due to the limitation imposed upon the method by the fact that echoes cannot be reflected from a given altitude unless the density exceeds that found at lower altitudes. The early results of Seddon and Jackson, who used a rocket-borne two-frequency radio propagation experiment, showed that the ionization is not concentrated in layers but rather is significant at all altitudes. Because of their work, then, it is more appropriate to use the term "region" rather than "layer" in discussing subdivisions of the ionosphere. The work of Seddon and Jackson has been reviewed adequately by Ratcliffe (ref. 1) and will not be detailed here.

With the advent of the satellite age, new information has been made available for altitudes well above those previously studied. Therefore one can now discuss seriously the characteristics of low energy particles out to the interplanetary plasma, rather than limit the scope to the original classical altitude region (up to approximately 300 km) imposed by the limitations of the ionosonde technique. It already is appropriate to consider the upper F region, the helium ion region, and the protonosphere as subdivisions of the ionosphere to be added to the classical D, E, F1, and F2 regions.

The principal purpose of this report is to compare theories of formation for each iono-

spheric region with existing spaceflight observations. When this is accomplished, it will be seen that one is left with inadequacies that justifiably require continuing consideration of the conflicting theoretical models which have been proposed. These inadequacies also invite the generation of new theoretical models, and are a measure of the vast program that remains to be accomplished, not only in the form of additional spaceflight observations but also in the form of supporting theoretical and laboratory research.

THE D REGION UNDER QUIET SOLAR CONDITIONS

The lowest altitude region where a significant number of free electrons are found lies between 50 and 85 km. Because of the relatively high gas densities, this D region is characterized also by high collision frequencies between the electrons and the neighboring neutral constituents. In these collisions, electromagnetic energy is transferred irretrievably to the neutral gas so that the region acts as a strong absorber of radio waves. Measurements of D region electron concentration are very difficult to make with ground-based techniques. These have, however, provided estimates for daytime conditions of 10^3 electrons/cm^3 near 80 kilometers.

The most favored theory of the formation of the daytime D region during conditions of low solar activity is that proposed by Nicolet and Aikin (ref. 2). The end result of their hypothesis is illustrated in figure 11–1 in the form of the altitude dependence of electron (n_e) and positive ion (n_+) concentrations. At altitudes below 70 km (dashed portion of the curves), cosmic rays are the principal radiations causing ionization and the diatomic ions of nitrogen and oxygen probably exist in greatest abundance. Between 70 and 85 km (broad portion of the curves) Lyman α radiation (1215.7Å) is the dominant ionizing agent even though it can only act on a minor constituent, nitric oxide. In the base of the E region (85–100 km), X-radiation is an important ionization source with O_2^+ and NO^+ believed to be the major ionic constituents. There is a high probability that newly formed electrons can attach to neutral particles to form negative ions only in the lower part of the D region. The predicted negative ion abundance is the difference between the theoretical n_e and n_+ curves in figure 11–1.

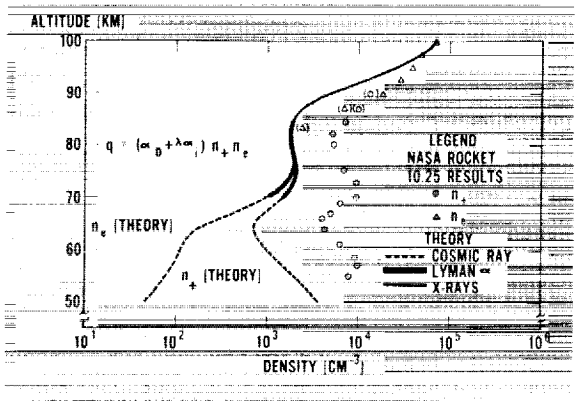

FIGURE 11–1.—The daytime D region under quiet solar conditions.

The model of Nicolet and Aikin was calculated from an expansion of the following conventional equation of ionization:

$$q = \alpha n_e^2, \qquad (1)$$

where q is an equivalent production of electrons and α is an effective loss process coefficient. The expansion includes the differing effects of all possible ionizing sources and several loss processes. For a single source and a single ionizable constituent an equation of the following form results:

$$q = (\alpha_d + \lambda\alpha_i)\, n_+ n_e, \qquad (2)$$

where α_d denotes the loss coefficient for recombination of positive molecular ions with electrons, α_i denotes the loss coefficient for recombination of positive with negative ions, and λ is the ratio of negative ions to electrons. The value of λ is computed from the probability of electron loss in the formation of negative ions and the effect of solar radiation in photo-detaching electrons from the ions. The charged particle densities are computed from spaceflight observations of cosmic rays and solar radiation, laboratory measurements of the loss processes, and an assumed model of the number density of ionizable constituents.

Principally because of the low ratio of charged particle to neutral gas density, electron densities in the D region are difficult to measure

from a rocket, although refinements of existing experiments should soon provide valid results. Some rocket data on the positive ion characteristics are available and these are consistent qualitatively with the Nicolet-Aikin model. Bourdeau, Whipple, and Clark first measured the positive ion conductivity (σ_+) with a rocket-borne Gerdien condenser and confirmed cosmic radiation as the ionizing agent up to 60km (ref. 3). Positive ion densities can be estimated from the observed conductivity according to

$$\sigma_+ = n_+ e k_+, \tag{3}$$

Where e is the elementary charge and k_+ is the ion mobility, whose altitude dependence is measurable in the laboratory.

More recently, Smith (ref. 4) obtained a positive ion conductivity profile by use of a *dc* probe analogous in principle to the Gerdien condenser. The positive ion densities which he computed from the observed conductivity are plotted in figure 11–1. At an altitude of approximately 90 km the theory of the experiment relevant to positive ion characteristics breaks down. Above this altitude the same device acts a Langmuir probe, thus permitting a measurement of electron density. Converse to the positive ion determination, the Langmuir probe theory becomes inadequate below about 85 km. For these reasons, the electron and positive ion density values in the region of overlap (85–90 km) are bracketed to indicate the possibility of second-order errors. Except for the lowest altitude point, the shape of the experimental charged particle density profile is similar to that of the Nicolet-Aikin model. It favors the concept of three separate ionizing sources in the 50–100 km region. The individual accuracies of the electron and positive ion densities are believed high enough in the 85–90 km region to conclude that negative ions become unimportant in the daytime ionosphere above 85 km. The general excess of the experimental positive ion densities over the theoretical estimates may be interpreted as an altitude invariant error either in the ion mobility used for the experimental result or in one of the assumed theoretical parameters.

Popoff and Whitten (ref. 5) have challenged the Nicolet-Aikin model by proposing X-rays as the principal ionizing agents above 70 km. Nicolet and Aikin did consider X-rays using published data from Friedman and others. Popoff and Whitten used a flux value, integrated over the responsible wavelength region (2–8Å), of 10^{-3} ergs/cm^2-sec. Aikin (ref. 6) considers this flux value either as typical of conditions of a disturbed sun or as an upper limit for a quiet sun during the solar maximum. Recent data from the Orbiting Solar Observatory I (W. White, private communication) and the Ariel I satellite (ref. 7) are consistent with Aikin's conclusions.

It is believed, but not generally accepted, that the Lyman α flux is relatively constant with the solar condition and throughout a solar cycle. The X-ray flux, on the other hand, varies by a factor of 1000 (ref. 8). The question of the relative influence of these ionizing agents on the normal daytime D region will not be resolved with certainty until valid charged particle density profiles of both signs are measured simultaneously with the appropriate cosmic ray, Lyman α, and X-ray fluxes, as well as the number density of the ionizable constituents. It as possible that such correlative data will show that the two source candidates for the 70–85 km region will alternate in relative influence depending on the exact solar condition. It is also possible that the normal D region is extremely more complicated than that described above. For example, Whipple (ref. 9) has calculated ion densities from the original conductivity profile and attributes a resulting large decrease at altitudes between 70 and 80 km to ionic diffusion to dust which may be trapped temporarily in this region of temperature inversion shortly after meteor showers. This sort of loss mechanism has not been considered in the previously described theoretical models.

When one considers that the theoretical and experimental data presented in figure 11–1 are not totally consistent and furthermore that they are representative of a particular latitude, a specific season and time of day, and a unique part of the solar cycle, it is realized quite easily that the study of the D region has just begun. The geographic and temporal coverage must be extended by a vast number of rocket flights, domestically and on an international scale.

Before this can be meaningful, however, new experiments are needed. Valid methods of measuring electron density below 80 km still escape us primarily because of the low ratio of charged to neutral particle density. There are no existing spectrometers for measuring either the ion or the neutral composition in this region of relatively high pressure. For example, the very existence of the minor constituent, nitric oxide, which the Nicolet-Aikin theory requires has not been verified experimentally. This lack forces the theoretician to make unverified assumptions in estimating both the production and the loss rate of electrons. There remain inconsistencies in the absolute values and time variations of the ionizing radiation. As for the loss coefficients which are measurable only in the laboratory, we are faced with orders of magnitude disagreement between investigators for some important reactions. On the theoretical side, additional loss mechanisms, particularly that suggested by Whipple, bear further investigation.

THE D REGION UNDER DISTURBED SOLAR CONDITIONS

During periods of high solar activity, the D region is characterized by enhanced ionization, with associated strong attenuation of electromagnetic waves causing radio blackouts. There are many phenomena associated with solar flares which increase the normal D region electron densities by up to two orders of magnitude. A comparison of the amount of enhanced ionization for disturbed solar conditions is made with the quiet sun model in figure 11–2.

Simultaneously with the appearance of a flare, radio absorption is observed in the D region on the sunlit side of the earth for periods lasting up to approximately one hour. This particular event is called a Sudden Ionospheric Disturbance (SID). Friedman, et al. (ref. 10) made rocket flights into such an event and observed abnormally high X-ray fluxes penetrating as low as 30 km. It has been observed that not only does the overall intensity increase but also that the spectrum in the 2–8Å region "hardens" in that the flux per unit wavelength is much broader than the quiet sun spectrum. Nicolet and Aikin (ref. 2) have

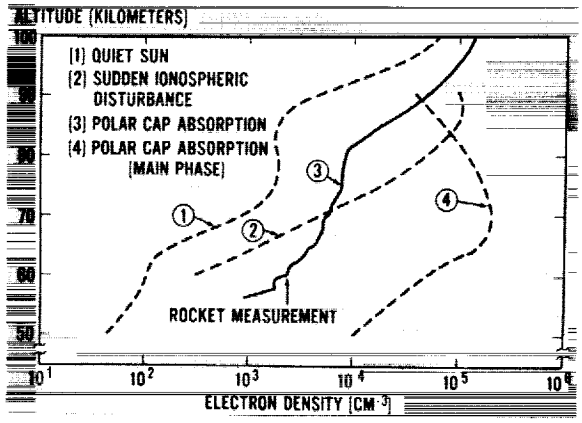

FIGURE 11–2.—Comparison of the D region under quiet and disturbed solar conditions.

used these observations to infer an electron density profile for the SID condition (curve 2 of fig. 11–2) in a manner similar to the development of the quiet sun model. Here, the influence of cosmic ray and Lyman α radiation becomes minor, the secondary layer in the 65–80 km region disappears, and the profile is characterized by overall enhancement and a monatonically increasing electron density.

A second type of ionospheric storm is associated with active auroral and magnetic disturbances and predominates at night. The ionizing agents are believed to be energetic particles comprising corpuscular emission from the sun. This belief is founded on the observation that D region absorption occurs some 21 hours after the appearance of a flare, an interval corresponding to the sun-earth transit time for these particles. During the storm, D region electron densities increase to values high enough that echoes are observed on ionosondes. Layers appear at 90 km during weak geomagnetic activity and as low as 70 km for the more active events.

A third type of disturbance occurs at auroral latitudes. These phenomena, called Polar Cap Absorption (PCA) events, are produced by energetic protons emitted from the sun during certain solar flares. Here echoes are observed from ionosondes at altitudes as low as 60 km. The phenomenon has been the subject of considerable study during the past few years. Most recently Maehlum and O'Brien (ref. 11) have proposed a semi-quantitative time history

of the D region electron density profile during a PCA by inserting proton fluxes observed on the Injun satellite as the source function in an expansion of the conventional equation of ionization. One of these profiles (curve 4 of fig. 11–2) coincides with the peak of the 27.6 mc cosmic radio noise absorption (17 db) observed at College, Alaska. Kane and Jackson (ref. 12) performed a rocket measurement of the D region electron density profiles (curve 3 of fig. 11–2) during a less active phase of a PCA event (3 db absorption at 30 mc). This compares favorably in shape but is generally less enhanced than that proposed by Maehlum and O'Brien during an interval when the observed radio absorption also was 3 db.

The status of our knowledge of the altitude distribution of charged particles for the multiplicity of disturbed conditions is exemplified by the fact that the dashed curves in figure 11–2 are speculative. We have some information on the ionizing radiation. The speculation starts with the absence of observational electron density information during special events and necessarily includes a model of the ionizable constituents which have not been measured. Additionally, a new set of loss coefficients, depending on the reaction of the ionizable constituents with energetic particles rather than ultraviolet and X-ray radiation, need to be measured in the laboratory.

THE ION CONTENT OF THE LOWER IONOSPHERE

To a high degree of probability, the predominant ionizing sources of the E and F region for quiet solar conditions at mid-latitudes are solar ultraviolet and X-ray radiations. If one knows the altitude dependence of the number of incident photons at each wavelength, of the densities of the individual neutral constituents, and of the absorption and photoionization cross sections of these constituents at each wavelength, it is possible to compute the rate at which different ion species are formed. Few of these parameters are known. There are available some altitude profiles of the photon fluxes as a function of wavelength but only for limited latitude and temporal conditions. Results from rocket-borne neutral gas spectrometers reported to date are extremely controversial, principally because recombination effects within the instruments distort the gas under study from its ambient condition. Thus, our understanding of the composition of the neutral gas is somewhat speculative. Another serious problem is that some of the absorption and photoionization cross sections are not known to an order of magnitude and others have not yet been investigated.

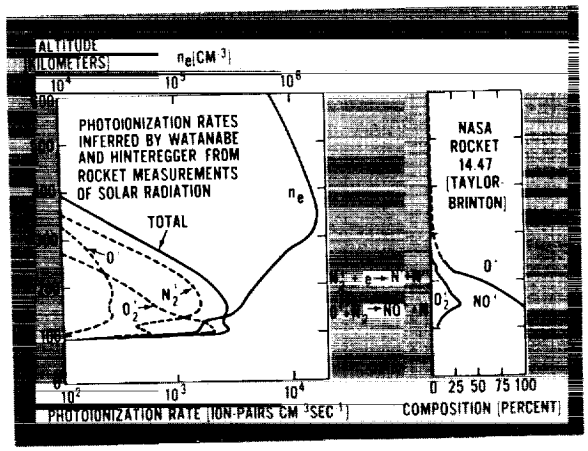

FIGURE 11–3.—Production and actual abundance of ions in the lower ionosphere.

The most recent estimate of the altitude dependence of the rate at which various ions are produced was made by Watanabe and Hinteregger (ref. 13) and is illustrated in the left-hand side of figure 11–3. They hasten to point out that in view of the uncertainty in our knowledge of the neutral atmospheric composition and of the pertinent cross sections, the curves are suggestive rather than quantitative. Even if the production rates were known, the problem of explaining the detailed altitude distribution of the electron density, also illustrated in the left-hand side of figure 11–3, is extremely complex.

The chemical complexity of the ionosphere can be demonstrated by comparing a rocket measurement (ref. 14) of the actual ion abundance (right-hand side of figure 11–3) with the inferred rates of production. It is seen, for example, that even though the diatomic nitrogen ions (N_2^+) are expected to be produced in great quantities, the spectrometer results show that they exist as an extremely minor charged constituent. The most likely reason is that N_2^+ ions dissociatively recombine almost as quickly

as they are produced. As a second example, it is seen that the spectrometer observations show NO^+ to be one of the predominant ion species below 200 km even though they are not formed as a direct result of solar radiation. The most likely process leading to the NO^+ abundance is the reaction of monatomic oxygen ions (O^+) which are directly produced with molecular nitrogen.

Considering only the two reactions indicated in figure 11–3 greatly oversimplifies the mechanisms by which the various ionospheric regions are formed. There are many reactions that need to be studied in the laboratory, including ion-atom interchange, charge exchange and dissociative recombination, to name a few. Exhaustive lists of the important reactions have been prepared (ref. 15) but there is no assurance that any of these lists are complete.

It is important to emphasize the need for a long range program of simultaneous vertical-sounding rocket observations of the solar radiation, neutral gas parameters, and charged particle characteristics. It is just as important to underline the need for supporting theoretical and laboratory research. When such a long range program has led us to universally accepted solutions for the continuity equation, it should be possible to predict the state of the ionosphere below an orbiting observatory which monitors only ionizing radiations.

THE DIURNAL VARIATION OF THE E REGION

The altitude region arbitrarily assigned to the E region lies between 85 and 140 km. Most textbooks favor a theory of E region formation based on general ionization of air by soft X-rays, yet Hinteregger and Watanabe (ref. 16) have recently disputed this hypothesis on the basis of more refined measurements of the solar ultraviolet radiation. The rocket ion spectrometer work of Johnson, Meadows, and Holmes (ref. 17) first showed that the major ionic constituents are O_2^+ and NO^+. The pioneering effort of Seddon and Jackson with a rocket-borne radio-propagation experiment showed that the electron density in the daytime behave with altitude in a manner similar to that illustrated in figure 11–4. The major discovery of this work was that, in terms of the electron density distribution, the F region is a continuation of the E region. Considering the daytime electron density profile shown in figure 11–4, we can see that a ground-based ionosonde would show reflections only up to an altitude of about 105 km and thus is unable to define the electron density distribution between that altitude and the base of the F region.

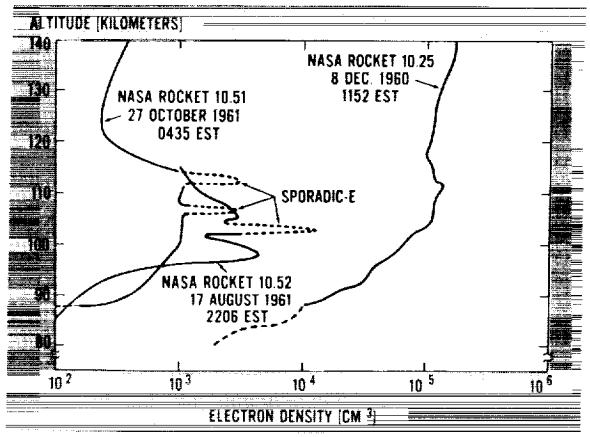

FIGURE 11–4.—Diurnal variation of the E region.

It is important to pause here and dissolve a popular misconception that spaceflight experiments are difficult to conceive and implement. The experimental method used to obtain the sets of data illustrated in figure 11–4 consisted of telemetering the current to the nose tip of a rocket as a function of a variable potential applied between that electrode and the main rocket body. In obtaining the end result, it is a more challenging task to apply kinetic theory and derive the desired charged particle parameter from the measured current than to implement the experiment.

Until very recently, there have been no observations of nighttime E region ionization because neither the ground-based ionosonde nor the rocket-borne propagation experiments are sensitive enough. All the rocket data illustrated in figure 11–4 were obtained by use of a dc probe (ref. 4 and 18).

Two nighttime electron density profiles are illustrated in figure 11–4, one obtained in the early evening hours and the other close to local sunrise. The general decay in the average electron density of about two orders of magnitude from the daytime condition is what would be

expected from a limited knowledge of the recombination coefficients. Both of these profiles show deep valleys of ionization above 110 km. The resulting ledge of ionization at altitudes of about 100–110 km are suggestive of a nighttime source of ionization. These valleys have been observed also by Japanese investigators (ref. 19), who used a rocket-borne radio-frequency oscillator based on the principle that a unique resonance is observed at the plasma frequency.

One anomaly which is observed quite frequently in both the daytime and nighttime E region is the sporadic-E layer. These are shown as dashed perturbations on the two nighttime profiles in figure 11–4. Rocket experiments have defined this condition, which to an ionosonde constitutes reflection at a constant virtual height, as enhanced ionization confined to a narrow altitude region of less than one kilometer. Consequently, the term "layer" is appropriate in defining this anomaly. There perhaps are many mechanisms producing sporadic-E. One of the likely causes is mechanical redistribution of the electrons from the regions above and below induced by wind shear. An extremely interesting exercise soon to take place will consist of the simultaneous launchings of two rockets, one instrumented for ionospheric studies and the other to measure the wind vector by the sodium release method. Should the sporadic-E layer and a pronounced wind shear coincide precisely in altitude at the same time, this hypothesis will have been demonstrated at least from an empirical point of view.

THE FORMATION OF THE F2 PEAK

The altitude region generally assigned to the lower F region lies between 140 and about 300 km. As illustrated in figure 11–3, there is an inflection point at about 140 km in the otherwise monotonically increasing electron density. For this reason the F1 and F2 subdivisions have been invoked. As a result of ground-based ionosonde investigations, it has long been established that the maximum electron density occurs at about 300 km. Until the satellite age, the region above this altitude was open to speculation.

The most favored theory of the formation of the F2 peak is illustrated by comparing a measured altitude dependence of electron density (ref. 20) with the rate of electron production inferred by a Watanabe and Hinteregger. This comparison is shown in figure 11–5. It is

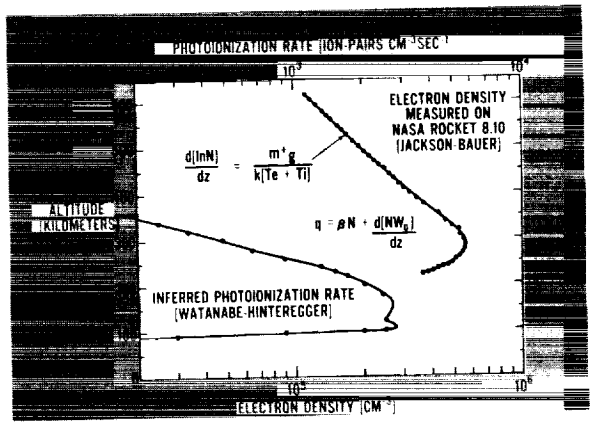

FIGURE 11–5.—The formation of the F region.

obvious immediately that the altitude of maximum electron density lies considerably above that at which the production rate is highest. This perhaps is best explained by considering the following simplified form of the continuity equation: corresponding to quasi-equilibrium.

$$q=\beta n_e+\frac{d(n_eW_D)}{dz}, \qquad (4)$$

where q is the production rate. The first term on the right-hand side is representative of an attachment-like loss mechanism, whereas the second term defines change in electron density by a diffusion process. In the region up to the $F2$ peak the loss by an attachment-like process predominates. Because this loss rate decreases more rapidly with altitude than does the production rate, the electron concentration increases up to its maximum value. At the $F2$ peak the diffusion term begins to predominate and the electron density begins to decrease. The diffusion mechanism is caused by gravitational forces acting upon the ions which, by coulomb attraction, cause the electrons to diffuse downward. At altitudes of about 400 km and above, both the production and loss processes become minor factors. As a result of diffusion, the

672058 O-63—3

electron density distribution in this region corresponds to hydrostatic distribution as follows:

$$\frac{d(\ln n_e)}{dz}=\frac{m_+ g}{k(T_e+T_i)}, \qquad (5)$$

where m^+ is the ionic mass, *te* and *ti* the electron and ion temperature respectively z is the altitude, g the acceleration of gravity, and k is Boltzmann's constant.

It should be emphasized that what has been presented is a favored theory for the formation of the $F2$ peak which is not universally accepted. Some investigators have proposed models without resorting to the diffusion process, by invoking loss mechanisms associated with minor ionic constituents. Such trace constituents have been observed on spacecrafts carrying ion spectrometers. The exact solution of the continuity equation for the region near the $F2$ peak has been the subject of considerable investigation and yet is not resolved satisfactorily. Furthermore, all theoretical models insert only solar ultraviolet flux into the production function. Yet, as a result of satellites designed to study the Van Allen belts, large fluxes of quasi-energetic particles which could provide an additional ionization source have been observed at some geographic locations in the upper ionosphere.

THE HELIUM ION LAYER AND THE BASE OF THE PROTONOSPHERE

As shown in Equation 5, the electron density at altitudes of about 400 km and above is governed by the ionic composition and the atmosphere temperature. Rocket-borne spectrometer data, typically represented in figure 11–3, showed that 0^+ ions begin to predominate at an altitude of about 200 km. It was later established by the Sputnik III (ref. 21) and Explorer VIII satellites (ref. 22) that this particular constituent was dominant up to 1000 km for a daytime ionosphere during the middle of the solar cycle. It generally was hypothesized that a direct transition from oxygen to hydrogen ions would take place just about 1000 km until Nicolet (ref. 23) suggested that helium is an important neutral constituent of the upper atmosphere. He based this suggestion on observations of drag on the Echo I satellite. There is now direct and indirect evidence that ionized helium plays an important role in controlling the electron density in the upper ionosphere.

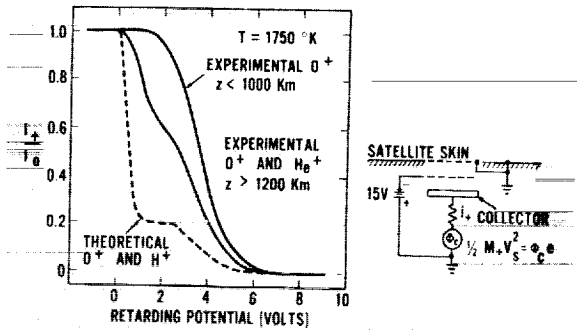

FIGURE 11–6.—Direct detection of helium ions from the Explorer VIII Satellite.

The first direct evidence was provided by a retarding potential experiment flown on the Explorer VIII satellite (ref. 24). This experiment is illustrated schematically in figure 11–6 together with the experimental observations. The sensor consists of three electrodes concentrically arranged in planar geometry. As a result of the negative bias applied to the inner grid, the collector reports to the telemetry system only that current which is due to positive ions flowing from the medium under study into the sensor. Because the satellite velocity exceeds the thermal velocity of the ions, their kinetic energy relative to the spacecraft is governed by their mass (M_+) and the known satellite velocity (V_s). This kinetic energy can be related to the potential energy, due to a known retarding potential (Φ_c) applied to the collector, by

$$\frac{M_+ V_s^2}{2}=\phi_c e. \qquad (6)$$

Because the thermal velocity of the ions cannot be neglected completely, the instrument functions as a "poor man's ion spectrometer" in that the ion resolution is coarse.

The interpretation of the experimental volt-ampere curves from the Explorer VIII satellite is summarized in the left-hand side figure 11–6. The predominant constituent can be

identified either from the potential required to retard half of the ions or from the shape of the curve, in accordance with the theoretical work of Whipple (ref. 25). For daytime conditions during the active life of the satellite (November, 1960), it was observed that O^+ ions predominated up to 1200 km but that helium ions were most abundant from 1200 km up to maximum observational altitude (1600 km). The average daytime electron temperature observed on Explorer VIII during this interval was 1800°K (ref. 26).

The first indirect evidence for a helium ion layer was reported by Hanson (ref. 27) using an ion density profile obtained by Hale (ref. 28). From the same data Hanson also reported the detection of the base of the protonosphere at an altitude of 3400 km. The atmospheric temperature deduced from the scale height of the electron-ion gas was 1600°K. Hanson also suggested that the thickness of the helium ion layer should be relatively invariant with diurnal time. On the other hand, Bauer (ref. 29) theoretically demonstrated that there is a diurnal variation.

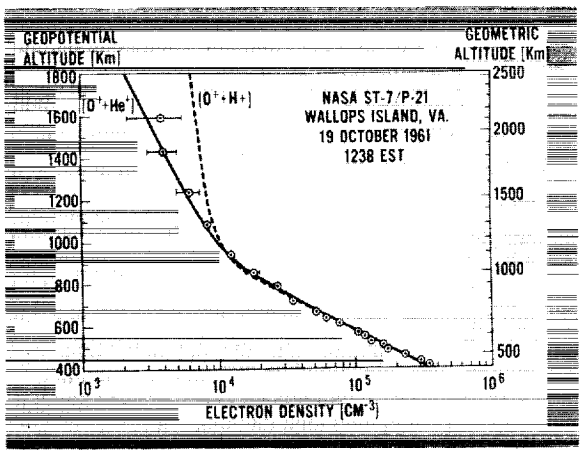

FIGURE 11–7.—Indirect detection of helium ions from vertically launched Scout rocket.

The indirect method of determining the ionic composition is illustrated in figure 11–7. The solid and dashed lines are theoretical predictions of the electron density distribution. They were computed by an expansion of Equation 5 which included more than one ionic constituent, and with the assumption that the atmospheric temperature is constant with altitude. The circles represent electron densities obtained experimentally by Bauer and Jackson (ref. 30) using a radio-propagation technique. The right-hand ordinate is true altitude and the left-hand ordinate is a reduced altitude scale which takes into account the change in the acceleration due to gravity. It is seen that the experimental data are consistent with a theoretical curve for a binary mixture of oxygen and helium.

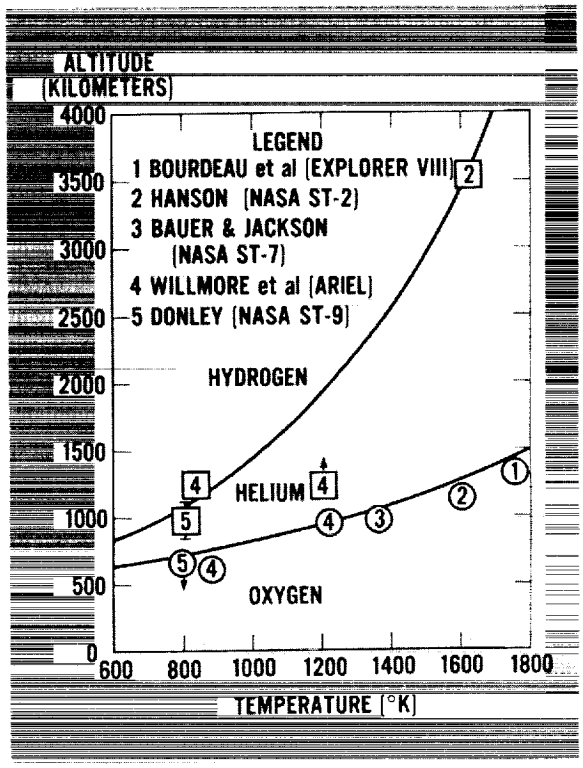

FIGURE 11–8.—Ion transition altitude as a function of atmospheric temperature.

Most observational data on the ionic composition support Bauer's suggestion of a strong dependence of the thickness of the helium ion layer on the atmospheric temperature, particularly his most recent theoretical model (ref. 31). This predicted thickness as a function of the atmospheric temperature is given by the separation of the solid lines in figure 11–8. The circles represent experimental observations of the altitude at which the helium and oxygen ions exist in equal concentrations. The squares, also experimental, are the altitudes at which the helium and hydrogen ions have the same num-

ber densities. The data sets 1, 2, and 3 were discussed above. A significant contribution has resulted from the Ariel I satellite (ref. 32). The experimental approach used on Ariel I is a much improved version of the retarding potential experiment. During the time of these observations (May, 1962), helium was detected as low as 600 km for a nighttime condition and at about 900 km during the daytime. For the latter condition, protons were not observed up to the apogee altitude (1200 km). However, they were detected at this altitude during nighttime passages. The last set of observations are by Donley (to be published) who used the direct and indirect methods simultaneously on a Scout rocket launched into the nighttime ionosphere.

The ionic composition of the upper ionosphere could be more variable than indicated by figure 11–8. It should be recognized that the observational data was obtained only at low latitudes. Secondly, some rocket flights have been made at night into this region where the detection of helium ions has not been reported (ref. 33). This could either be due to a larger temperature dependence than indicated in figure 11–8 or to experimental inadequacies. A wider latitudinal coverage is required. More importantly, the altitude region above 4000 km has yet to be explored for thermally charged particles by spaceflight experiments. The altitude region up to 10,000 km is being investigated by ground-based radar backscatter apparatus (ref. 34).

IONOSPHERIC TEMPERATURES

The temperature of the neutral gas (T) has been the subject of considerable study. It is generally accepted that this temperature becomes quite independent of altitude above 300 km. It will be the purpose of this section to compare observations of charged particle temperatures with reference neutral atmospheres to introduce additional questions in the already conflicting theories of heat and ionization sources in the upper atmosphere. This can best be accomplished by limiting the discussion to altitudes above 450 km where the electron temperature (T_e) is nearly equivalent to that of the neutral gas, (ref. 35), although this is not universally accepted.

Two types of observations are available. The first method involves the use of Langmuir probes to measure T_e directly. The second method is indirect. Referring to Figure 11–5, we see that if the ionic composition is known and if one has an accurately measured charged-particle profile it is possible to compute the sum of the electron and ion temperatures. This sum is related to the neutral gas temperature by $T=(T_e+T_i)/2$.

It is known that in the isothermal altitude region the neutral gas temperature varies considerably with diurnal time and the solar cycle. This variation can be correlated with solar decimeter flux which is observed at the earth and which serves as an index of solar activity. Neutral gas temperatures have been estimated from observations of satellite drag. It should be noted, however, that it is the atmospheric density, not temperature, which is directly obtained from satellite drag. The temperature is computed from the observed density and an assumed neutral gas composition. As emphasized previously, the latter parameter represents a major observational gap. It would be expected that if the absorption of solar ultraviolet radiation were the only heating acting on the atmosphere, then the maximum temperature on a given day would occur near sunset. What is observed is that the maximum density occurs in mid-afternoon. Some investigators imply that the time of maximum density corresponds to the time of maximum temperature and then reason that because of the phase shift from sunset to mid-afternoon an additional heat source must be introduced. This same hypothesis is used to explain observed seasonal variations of atmospheric density. One heat source that has been suggested (ref. 36 and 37) is corpuscular radiation associated with the solar wind which should not be latitudinally dependent. The charged particle temperature observations are not completely consistent with these reference atmospheres. It is not known with certainty whether this is because of a lack of temperature equilibrium or of inadequacies either in the neutral gas models or the charged particle temperature measurements.

Langmuir probes flown on the Explorer VIII satellite showed a diurnal variation of the electron temperature from 1000°K at night up to

1800°K during the day, at a time when the solar decimeter flux index was 150 (ref. 26). These measurements were not highly accurate (ref. 38). Furthermore, the lack of a tape recorder prevented the establishment of an exact diurnal variation and any observation of latitude dependence. More complete data are available now from the Langmuir probe experiment used on the Ariel I satellite which did contain a tape recorder. The results of Willmore, et al. (ref. 32) are reproduced as dashed lines in figure 11–9. Plotted are three curves of temperature

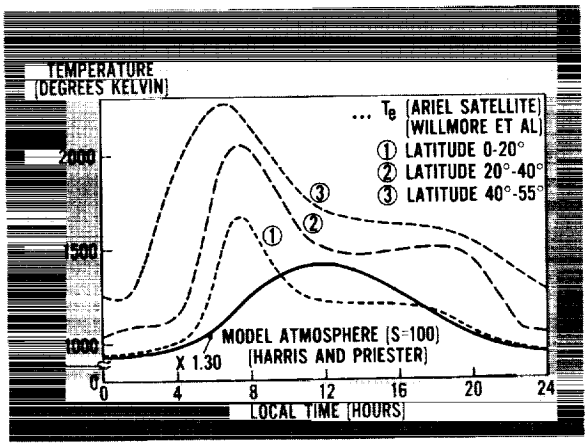

FIGURE 11–9.—Diurnal and latitudinal variation of exospheric temperature.

as a function of local time, each curve corresponding to a different latitude region. There are three important observations to be made from these data. First, there is a pronounced sunrise-effect which most probably represents a distinct departure from temperature equilibrium. As the sun rises, the electrons temperature would be expected to rise considerably above the neutral gas temperature. As a consequence, the sunrise effect should be ignored in the comparison with reference atmospheres.

The second important observation is that there is no pronounced peak in the mid-afternoon. On the assumption of temperature equilibrium during this part of the day, this would be inconsistent with the inferred diurnal temperature variation contained in reference atmospheres. As Willmore, et al. point out, the most important observation is the pronounced latitude effect, which they ascribe to energetic particle bombardment in the auroral region.

The Ariel I observations correspond to a solar decimeter fluz index of 100. The neutral gas model of Harris and Priester (ref. 36) for this level of solar activity is plotted in figure 11–9 for comparison with the Ariel I data. As Harris and Priester point out, the nature of satellite drag observations is such that the model is applicable only to low latitudes. Their entire temperature curve was multiplied by 1.3 to achieve agreement with the nighttime values at the lowest latitude of the electron temperature data. Rather good agreement would be achieved with the low latitude electron temperature curve if the atmospheric composition at high altitudes was assumed to vary with temperature in a fashion corresponding to that illustrated for ions in figure 11–8, rather than according to the variation which was used by Harris and Priester.

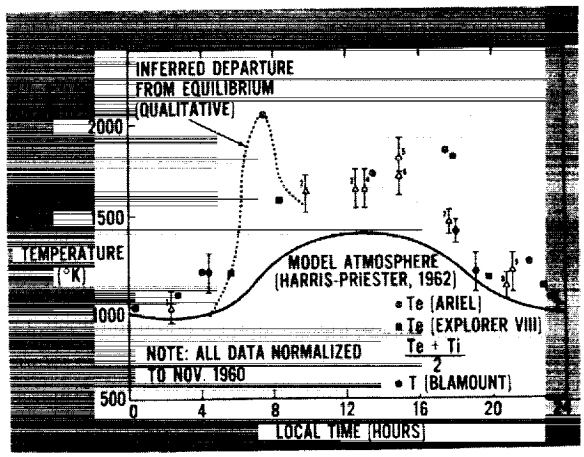

FIGURE 11–10.—Diurnal variation of exospheric temperature at mid-latitudes.

To give further confidence to the Ariel I electron temperature results, data taken from the curve corresponding to latitudes between 20 and 40 degrees are compared, in figure 11–10, with previous observations at these latitudes. The comparison necessitated normalizing all data to a given solar condition. This was accomplished by using the temporal variation suggested by Harris and Priester. It is seen that for the most part there is approximate agreement between the Ariel I and Explorer VIII electron temperature values and between these electron temperatures and values of $(T_e+T_i)/2$ obtained by the indirect method.

Furthermore, there also is approximate agreement between the charged particle temperature and values of the neutral gas measured by Blamont by the sodium release method (ref. 39 and 40). These all are suggestive of electron temperatures being approximately equal to the neutral gas temperature at altitudes above 450 km except during the sunrise period. However, the suggestion of temperature equilibrium implied by this comparison is based on the assumption that the normalization procedure for solar activity is correct.

It is important to note that the amplitude of the diurnal variation corresponding to directly measured temperatures is larger than that of the model atmosphere which is based primarily on satellite drag. The most likely reason is that the model atmosphere applies only to the near-equatorial region and thus the difference is latitudinal in nature. This is the same conclusion reached by the Ariel I investigators. It is also possible that T_e/T_i is latitude dependent.

If there is a latitudinal variation of T, the hypothesis of corpuscular radiation associated with the solar wind as a second source of heating becomes subject to doubt. A likely second source is auroral bombardment by energetic particles, as suggested by Willmore, et al. If this is so, a continuous ionization source at high latitudes, in addition to the solar ultraviolet and X-ray radiations, is also likely. The possibility of additional ionizing sources even for quiet solar conditions should expand an already large program of spaceflight observations, theoretical research, and laboratory investigations.

LIST OF REFERENCES

1. RATCLIFFE, J.: *Physics of the Upper Atmosphere.* Academic Press, 1960.
2. NICOLET, M., and AIKIN, A. C.: *The Formation of the D Region of the Ionosphere.* J. Geophys. Res., vol. 65, May 1960, pp. 1469–1483.
3. BOURDEAU, R. E., WHIPPLE, E. C., and CLARK, J. F.: *Analytic and Experimental Electrical Conductivity Between the Stratosphere and the Ionosphere.* J. Geophys. Res., vol. 64, October 1959, pp. 1363–1370.
4. SMITH, L. G.: *Electron Density Measurements by the Asymmetric Probe.* NASA Tech. Note, to be published.
5. POPOFF, I. G., and WHITTEN, R. C.: *D Region Ionization by Solar X-Rays.* J. Geophys. Res., vol. 67, July 1962, pp. 2986–2989.
6. AIKIN, A. C.: *The Formation of the Ionospheric D Region.* Proc. of the International Symposium on Equatorial Aeronomy, September 1962, to be published.
7. POUNDS, K., and WILLMORE, A. P.: *X-Ray Measurements on the Ariel Satellite.* Proc. of the International Conference on the Ionosphere, July 1962, in press.
8. KREPLIN, R. W., CHUBB, T. A., and FRIEDMAN, H.: *X-Ray and Lyman-Alpha Emission from the Sun as Measured from the NRL SR-1 Satellite.* J. Geophys. Res., vol. 67, June 1962, pp. 2231–2253.
9. WHIPPLE, E. C. JR.: *Direct Measurements of Ion Density and Conductivity in the D-region.* XI th International Astron. Congress, 1960, pp. 99–102.
10. FRIEDMAN, H., CHUBB, T. A., KUPPERIAN, J. E., KREPLIN, R. W., and LINDSAY, J. C.: *X-ray and Ultraviolet Emission of Solar Flares.* Ann. Geophys., vol. 14, 1958, pp. 232–235.
11. MAEHLUM, B., and O'BRIEN, B. J.: *Solar Cosmic Rays of July 1961 and Their Ionospheric Effects.* J. Geophys. Res., vol. 67, August 1962, pp. 3281–3288.
12. JACKSON, J. E., and KANE, J. A.: *Measurement of Ionospheric Electron Densities Using an RF Probe Technique.* J. Geophys. Res., vol. 64, August 1959, pp. 1074–1075.
13. WATANABE, K., and HINTEREGGER, H. E.: *Photoionization Rates in the E and F Regions.* J. Geophys. Res., vol. 67, March 1962, pp. 999–1006.
14. TAYLOR, H. A., and BRINTON, H. C.: *Atmospheric Ion Composition Measured Above Wallops Island Virginia.* J. Geophys. Res., vol. 66, August 1961, pp. 2587–2588.
15. AIKIN, A. C.: *Charged Particle Reactions of Importance in the Ionosphere.* Goddard Space Flight Center Rept. X-615-62-132, August 1962.
16. HINTEREGGER, H. E., and WATANABE, K.: *Photoionization Rates in the E and F Regions, 2,* J. Geophys. Res., vol. 67, August 1962, pp. 3373–3392.
17. JOHNSON, C. Y., MEADOWS, E. B., and HOLMES, J. C.: *Ion Composition of the Artic Ionosphere.* J. Geophys. Res., vol. 63, 1958, pp. 443–444.

18. SMITH, L. G.: *Rocket Measurements of Electron Density and Temperature in the Nighttime Ionosphere.* NASA Tech. Note, to be published.
19. AONO, Y., HIRAO, K., and MIYAZAKI, S.: *Positive Ion Density, Electron Density and Electron Temperature in the Ionosphere.* J. of the Radio Research Laboratories, vol. 8, 1961, pp. 453–465.
20. JACKSON, J. E., and BAUER, S. J.: *Rocket Measurement of a Daytime Electron Density Profile up to 620 km.* J. Geophys. Res., vol. 66, 1961, pp. 3055–3057.
21. ISTOMIN, V. G.: *An Investigation of the Ionic Composition of the Earth's Atmosphere Using Rockets and Earth Satellites.* Artificial Earth Satellites, vol. 2, 1962.
22. BOURDEAU, R. E.: *Ionospheric Results with Sounding Rockets and Satellites.* Proc. Second International Space Sciences Symposium, April 1961, pp. 554–573.
23. NICOLET, M.: *Helium, and Important Constituent in the Lower Exosphere.* J. Geophys. Res., vol. 66, March 1961.
24. BOURDEAU, R. E., DONLEY, J. L., WHIPPLE, E. C., and BAUER, S. J.: *Experimental Evidence for the Presence of Helium Ions Based on Explorer VIII Satellite Data.* J. Geophys. Res., vol. 67, February 1962, pp. 467–475.
25. WHIPPLE, E. C., JR.: *The Ion Trap Results in Exploration of the Upper Atmosphere with the Help of the Third Soviet Sputnik.* Proc. IRE, vol. 47 December 1959, pp. 2023–2024.
26. SERBU, G. P., BOURDEAU, R. E. and DANLEY, J. L.: *Electron Temperature Measurements on the Explorer VIII Satellite.* J. Geophys. Res., vol. 66, December 1961, pp. 4313–4315.
27. HANSON, W. B.: *Upper Atmosphere Helium Ions.* J. Geophys. Res., vol. 67, January 1962, pp. 183–188.
28. HALE, L. C.: *Ionospheric Measurements with a Multigrid Retarding Potential Analyzer.* J. Geophys. Res., vol. 66, pp. 1954.
29. BAUER, S. J.: *On the Structure of the Topside Ionosphere.* J. Atmos. Sci., vol. 19, May 1962.
30. BAUER, S. J., and JACKSON, J. E.: *Rocket Measurement of the Electron Density Distribution in the Topside Ionosphere.* J. Geophys. Res., vol. 67, April 1962.
31. BAUER, S. J.: *On the Thickness of the Helium Ion Layer.* NASA Tech. Note 1686 to be published.
32. WILLMORE, A. P., BOYD, R. L. F., and BOWER, P. J.: *Some Preliminary Results of the Plasma Probe Experiments on the Ariel Satellite.* Proc. of the International Conference on the Ionosphere, July 1962, in press.
33. ULWICK, J. C., and PFISTER, W.: *Spatial and Temporal Variations of Electron Density from an Orbiting Satellite.* Third International Space Science Symposium, May 1962, in press.
34. BOWLES, K. L., OCHS, G. R., and GREEN, J. L.: *On the Absolute Intensity of Incoherent Scatter Echoes from the Ionosphere.* NBS Journal of Research, Section D, in press, 1962.
35. BOURDEAU, R. E., and BAUER, S. J.: *Structure of the Upper Atmosphere Deduced from Charged Particle Measurements on Rockets and the Explorer VIII Satellite.* Third International Space Science Symposium, May 1962, in press.
36. HARRIS, I., and PRIESTER, W.: *Theoretical Models for the Solar-Cycle Variation of the Upper Atmosphere.* NASA, Tech. Note D–1444, August 1962.
37. JACCHIA, L. G., and SLOWEY, J.: *Accurate Drag Measurements for Eight Artificial Satellites; Atmospheric Densities and Temperatures.* Smithsonian Institution Astrophysical Observatory Report, No. 100, July 1962.
38. BOURDEAU, R. E., DONLEY, J. L., and WHIPPLE, E. C.: *The Ionosphere Direct Measurements Satellite.* NASA Tech. Note D–414, 1961.
39. BLAMONT, J.: *La Temperature de l' Ionosphere.* Proc. Second International Space Sciences Symposium, April 1961.
40. BLAMONT, J.: Private communication.

Particles and Fields Research in Space

By George H. Ludwig

DR. GEORGE H. LUDWIG *has headed the Fields and Particles Branch Instrumentation Section of the NASA Goddard Space Flight Center since 1960. Instrumentation for a number of spacecraft, including the recent Explorers X and XII was developed here. He is currently the project scientist for the 900 pound Orbiting Geophysical Observatory to be launched in 1963. Dr. Ludwig received the B.A. and M.S. degrees with a major in Physics in 1956 and 1959, respectively, and the Ph. D. degree in Electrical Engineering in 1960, all from the State University of Iowa. As a graduate research assistant to Dr. J. A. Van Allen, he developed most of the corpuscular radiation instrumentation for Explorers I, II, III, IV, V, VII, and project S–46. Explorers I, III, IV, and VII were successfully launched and led to the discovery of the high intensity trapped radiation. Dr. Ludwig is a member of Phi Beta Kappa, Sigma Xi, American Geophysical Union, Institute of Radio Engineers, and American Rocket Society.*

INTRODUCTION

Throughout the universe physical processes occur which result in the formation, ionization, and acceleration of matter. The motion of these charged particles results in the formation of magnetic and electric fields. The further interaction of these moving particles with other magnetic and electric fields results in their further acceleration. As a result, there exists a whole continuum of charged particles having energies from thermal to at least 10^{19} electron volts, and nuclear structures from that of hydrogen (single protons) to that of heavier materials (at least iron). And throughout regions as large as whole galaxies, there exist complex magnetic and electric fields. Until the coming of high altitude balloons and rockets, and the earth satellites and interplanetary probes, we were restricted to the study of the particles and fields which reached the earth through its modifying atmosphere and strong magnetic field, and to the study of secondary processes occurring far from the earth which produced radiations capable of reaching the earth. Two examples of such indirect observations are: (1) the study of the magnetic field fluctuations at the surface of the earth to deduce the existence of large electric currents (ring currents) in the high atmosphere; (2) the observations of radio signals which presumably are produced by synchrotron radiation of electrons contained in a Jovian high intensity radiation belt.

The new instruments of the space age allow us to conduct experiments within and outside the earth's modifying atmosphere and magnetosphere to learn more about these interesting phenomena.

This paper will summarize briefly our present state of understanding of the energetic charged particle populations in space and the characteristics of the magnetic fields which interact with them. For convenience, we shall begin with a discussion of the galactic cosmic rays, which are the largest scale phenomenon, and then proceed to solar cosmic rays, solar plasma, and the earth's geomagnetically trapped radiation which forms the Van Allen radiation belts.

672058 O-63—4

GALACTIC COSMIC RAYS

Galactic cosmic rays are those particles which are accelerated outside our solar system and arrive with kinetic energies greater than about 10 Mev per nucleon. Cosmic rays having energies as high as about 10^{19} electron volts have been detected. It seems difficult to imagine that these very high energy particles could be produced within our own galaxy, since their radius of curvature in the galaxy's magnetic field (which cannot be much stronger on the average than about 10^{-5} gauss) is of the order of the dimensions of the galaxy itself. Thus, it is presently believed that they arrive from other galaxies. Lower energy galactic cosmic rays certainly must originate from within our own galaxy. It is probable that at least some of them are produced initially by localized eruptions on the turbulent surfaces of stars, similar to those which produce the solar cosmic rays which we will discuss later. It is also probable that supernovae may be an important source.

These particles are then accelerated. Parker (ref. 1) has shown that within the framework of the present understanding of plasma dynamics, all particle acceleration mechanisms occurring outside of the laboratory are reducible to the Fermi mechanism (ref. 2, 3, 4) which is based on random particle collision with magnetic inhomogeneities. Insofar as comparisons can be made, the experimental results seem consistent with this Fermi type acceleration mechanism.

The features of the galactic cosmic rays which are most amenable to investigation are the energy and charge spectra, and the modulation of their characteristics with time. The study of the directional characteristics to ascertain their sources is not very fruitful because the directions of motion of the particles are changed by the very complex magnetic fields through which they pass, so that the flux is very nearly isotropic.

Charge Spectrum

The composition (or charge spectrum) of the primary cosmic radiation striking the top of the earth's atmosphere is reasonably well known at the present time (ref. 5, 6, 7). Briefly, 85% of the particles are hydrogen, 12% are helium, approximately 1% are in the carbon, nitrogen, and oxygen group, about 0.25% are in the lithium, beryllium and boron group, and 0.25% are neon and heavier. In this heavier group, nuclei of all charges up to and including iron ($Z=26$) have been identified. High energy electrons constitute 1 to 3% of the total flux (ref. 8, 9). Whether these electrons are of galactic or solar origin is not fully understood at the present time.

A detailed summary of the charge spectrum is given in table 12–I. There are two features of this charge spectrum which should be mentioned. First, the flux of lithium, beryllium, and boron is surprisingly high if we assume that these elements are extremely rare in the source region, as the table of stellar abundance would have us believe. These nuclei must be produced by fragmentation of heavier nuclei colliding with interstellar hydrogen nuclei. This, then, gives a measure of the average distance traversed by the galactic cosmic radiation before striking the earth. If we use presently available fragmentation parameters (ref. 7), this corresponds to a value of 4 gms/cm² or implies an average age of the particles of the order

TABLE 12–1.—*Relative Abundances of Multiply Charged Nuclei*

	He	*Li, Be, B*	*C*	*N*	*O*	*F*	*Ne*	$11 \leq Z \leq 18$
*Galactic Cosmic Rays	360	11	18	$\lesssim 8$	10	$\lesssim 1$	3	9
†Sun	?	<0.01	6	1	10	<0.01	?	1
*Solar Cosmic Rays	1250	0.3	6	$\lesssim 2$	10	<0.4	1.5	1.3

*The uncertainty in the values in this line varies from 10 percent to 30 percent.
†The uncertainty in the values in this line are of the order of a factor of 2.

of 10^7 years. The other interesting feature is the large flux of carbon, nitrogen, and $Z>10$. The observed values are 10 times greater than that expected from the known stellar abundances. At the present time, this is not understood but can perhaps be explained in terms of supernovae origin (ref. 10).

Energy Spectrum

In the high energy region ($E>3$ Bev) it has been observed that all charged components have energy spectra of the form

$$J(E)=\frac{Kz}{(1+E)^{\gamma}},$$

where $J(E)$ is the flux in particles/(m²-sec-sr) with kinetic energy $>E$, γ is a constant independent of Z, and $K(z)$ is a function of Z. $J(E)>0.5$ Bev) is typically 1800 particles/(m²-sec-sr) at solar maximum.

In the region 0.3–5 Bev it is observed that all charge components appear to display similar spectral forms when expressed in terms of rigidity ($R \propto p/Z$) where p is the momentum and Z is the charge of the particle. The differential energy spectrum shown in figure 12–1 displays a maximum in the region of 400 Mev per nucleon and extends down to at least 90 Mev per nucleon. In the region 90 to 200 Mev per nucleon Meyer and Vogt have found large increases, which they believe are due to solar cosmic rays (ref. 11). Data from Explorer XII do not show this increase; further work will be necessary before this disagreement can be explained.

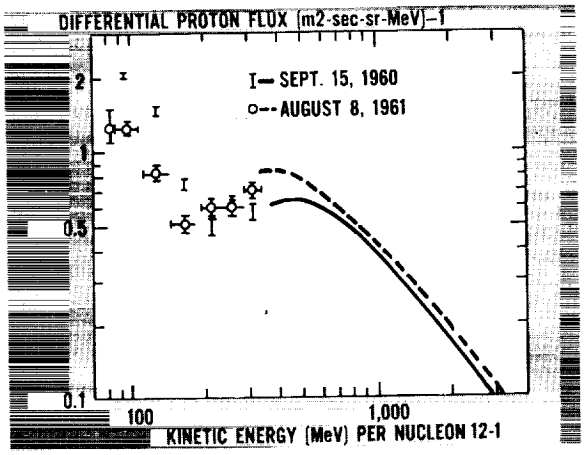

FIGURE 12–1.—Cosmic ray differential energy spectrum (ref. 11).

Modulation of the Galactic Cosmic Radiation

It appears reasonable to assume that the flux of cosmic rays incident on the solar system is constant. However, in the vicinity of the earth large modulations are observed which appear to be controlled by solar activity. The two most important types of modulation appear to be the 11 year variation and the Forbush or storm-type decrease. It was first noted by Forbush that the cosmic ray intensity varied inversely with solar activity over an 11 year cycle (ref. 12). Also, Forbush first observed the rapid world-wide decreases in cosmic ray intensity which are associated with some magnetic storms (ref. 13), generally following large type 3^+ solar flares. At present the best evidence indicates that the modulations are heliocentric and controlled by solar activity. The effects on cosmic rays can be summarized as follows (ref. 14):

(1) The proton and alpha particles (hydrogen and helium nuclei) ($R>1.0$ BV) similar forms of differential rigidity spectrum at solar minimum, and maintain the same relative form of rigidity spectrum throughout the solar cycle.

(2) The total intensity is smaller by a factor of 2 at solar maximum than at solar minimum, and the lower energy particles are modulated most. However, the low energy component is never completely removed.

(3) At low energies the form of the spectrum change appears to be the same for the 11 year cycle as for the Forbush decreases which have been observed.

The modulation effects are interpreted as being due to large scale variations of the solar magnetic field. Increases of the magnetic field strength near the earth result in the deflection of the lower energy particles before they penetrate this field to the position of the earth. This field arises from two sources. A relatively steady magnetic field is the result of the streaming of solar plasma from the sun, and is of the order of 5 to 10 gammas at the earth's orbit, where one gamma equals 10^{-5} gauss. Variations in this field result in the 11 year cycle. The Forbush, or storm decreases are caused by

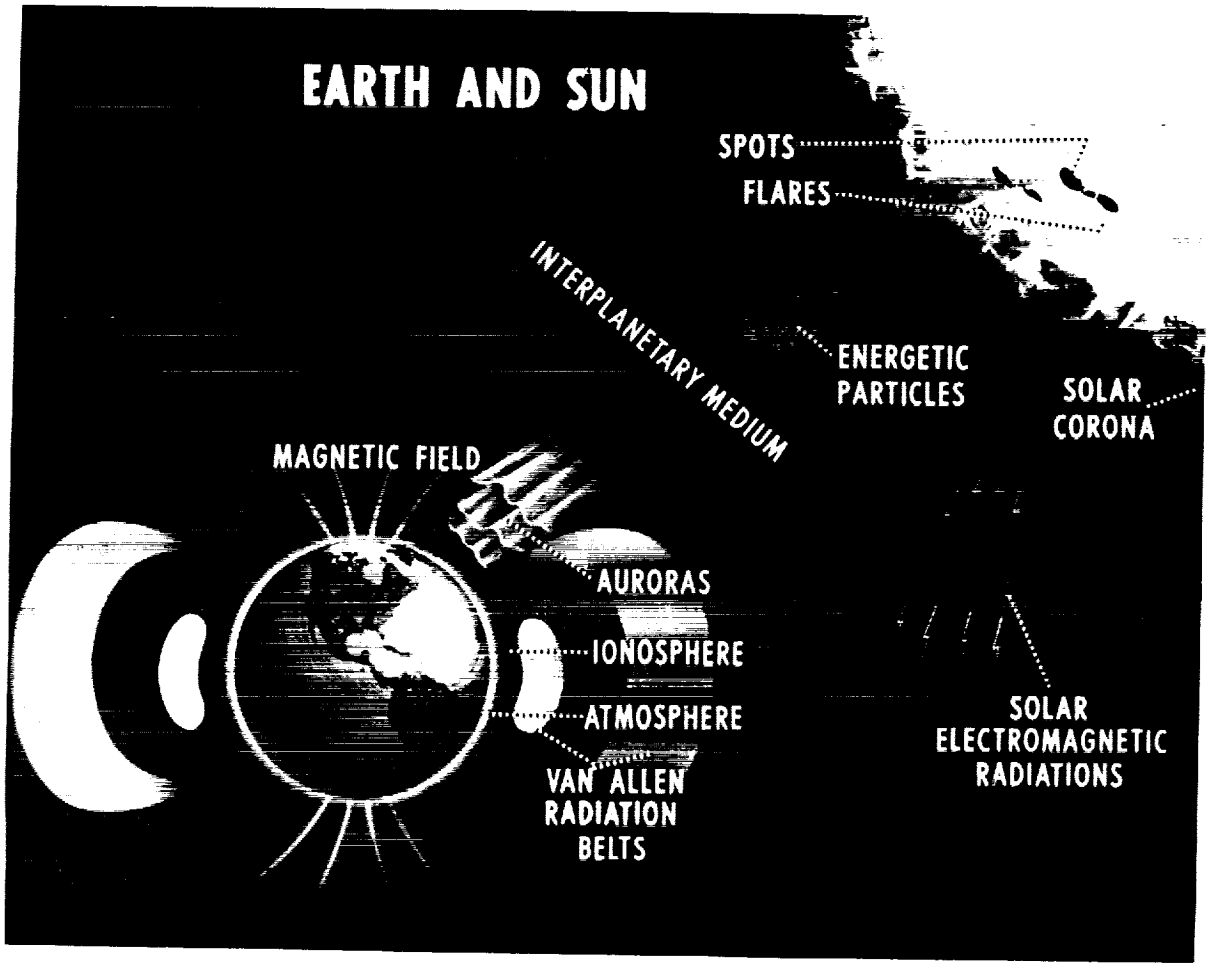

FIGURE 12-2.—Sun-earth phenomena.

somewhat more localized fields generated as a result of large solar flares.

SOLAR COSMIC RAYS

The surface of the sun boils in an active manner as the result of the continuous production of energy inside the sun. At times the surface becomes unusually turbulent and ejects clouds of charged particles and streams of radio, visual, x-ray, and gamma ray radiation into the space surrounding the sun (fig. 12-2). These solar eruptions are known as flares and the charged particles are known as solar cosmic rays.

When the flare is situated in the right position on the sun's surface, the clouds of particles are ejected in such a direction that they reach the earth and interact with its atmosphere. There they produce magnetic storms, radio blackouts, auroral displays, and other phenomena.

The streams of solar cosmic rays containing a large high energy content can be detected by sea level ion chambers and neutron monitors (ref. 15, 16). The development of the riometer (ref. 17) in 1957 provided an instrument which is sensitive to the effects of small fluxes (10 particles/(cm^2-sec-sr)) of incoming particles in the low energy region (10 to 100 Mev). There were at least a dozen events per year during the last solar maximum which were detectable by riometers (ref. 18).

The most detailed information about these solar cosmic rays has come from particle detectors flown on balloons, rockets, and spacecraft (ref. 19, 20, 21). Enough data have been obtained to give an indication of the sequence

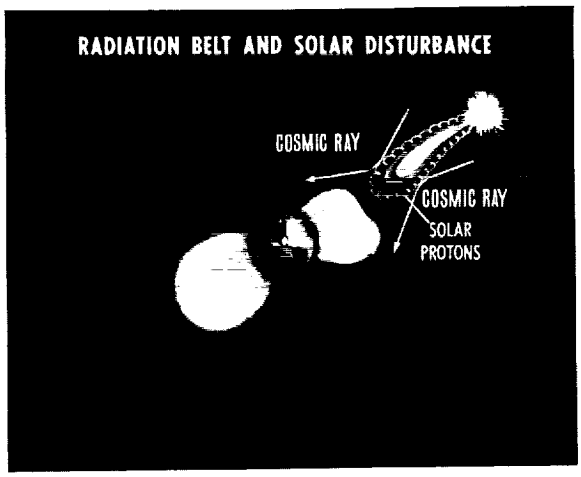

FIGURE 12–3.—Idealized solar proton event configuration, showing the solar proton cloud, the drawn-out field, and the effect on galactic cosmic rays.

of events occurring during these disturbances. When a solar flare occurs, a tongue of charged particles erupts from the sun's surface at a speed of from 1000 to 2000 kilometers per second (fig. 12–3). It takes about a day for this cloud to reach the earth. The charged particles drag along the lines of the solar magnetic field which become frozen into the cloud and forced to move with it according to Maxwell's laws. As the force lines become distended in this manner they lose their strength. However, the field is still strong enough at the distance of the earth to cause a partial screening of the galactic cosmic rays resulting in the Forbush decreases discussed earlier. Solar cosmic rays continue to arrive at the earth for several days after the initial encounter, presumably because of the storage of particles in this magnetic field.

The particle cloud advances outward from the sun at such a high speed that it must be proceeded by a shock wave. This shockfront may be the reason for the sudden-commencement characteristic of many magnetic storms. Parker (ref. 22) believes that this shock, resulting in a linked and strengthened magnetic field behind the advancing front, is the most important part of the solar storm process. The advancing shock wave and particles result in the geophysical phenomena mentioned earlier.

One of the most striking features of these solar cosmic ray events has been the variation from one event to another. In some events, the flux of protons above 20 Mev has exceeded 10^3 particles/(cm^2-sec-sr) for more than a day (ref. 20, 23, 24) and the total energy arriving at the top of the atmosphere of the earth for the whole event has been 10^4 ergs/(cm^2-sr), about the same order of magnitude as that for cosmic rays for a year. On the other hand, events which are more than a hundred times smaller than this have been seen (ref. 25, 26), and even smaller ones probably occur frequently and are not detected. The energy spectra also shows marked differences from one event to another. For example, at comparable times in the November 12, 1960, and the July 12, 1961, events (ref. 24, 27) the integral fluxes above 10 Mev were nearly the same, but above 100 Mev they differed by more than a factor of 300. In some events, the maximum low energy intensity occurred as early as two hours after the flare; whereas in others, it occurred as late as thirty or forty hours after the flare. In order to show some of the general characteristics of these events, the time variations of the integral fluxes above 20, 100, and 500 Mev are shown for three large events (ref. 28) in figure 12–4.

On the basis of the detailed study of these three events, there seems to be good evidence that the relative abundances of all elements having charges greater than one but less than about sixteen are nearly independent of energy. They are shown in table 12–I, along with the natural relative abundances existing in the sun, deduced from spectroscopic evidence for those elements. It is seen that the two sets of numbers are the same within uncertainties. Although the helium abundance in the sun cannot be determined by spectroscopic means, the relative abundance given in table 12–I for helium in solar cosmic rays is within the rather wide limits set by theoretical models of the sun.

The proton component has been observed to have a very different energy spectrum from the other components, probably because of its different charge to mass ratio. This has the effect that the relative abundance of the proton component is a function of velocity. For example, in one event the proton to helium ratio varied from about twenty at 40 Mev/nucleon to about three hundred at 120 Mev/nucleon.

It can be seen from table 12–I that the rela-

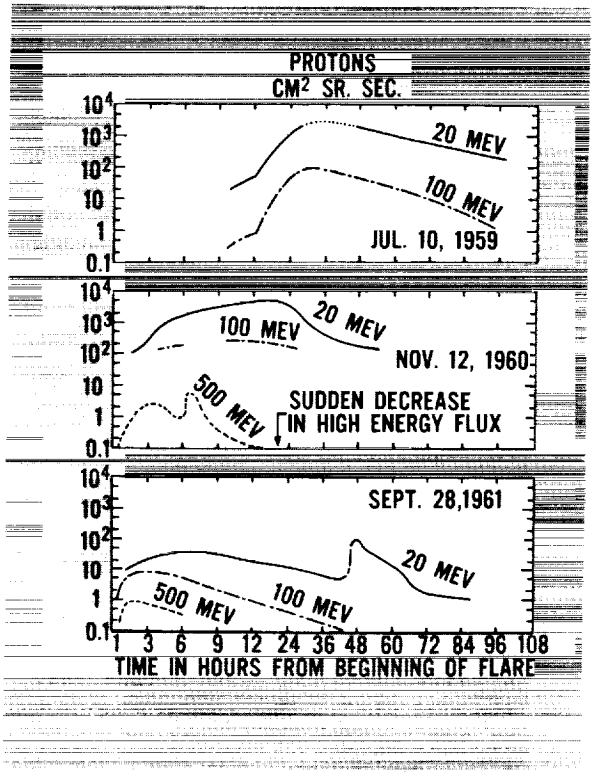

FIGURE 12–4.—Time variation of the integral flux above 20, 100, and 500 Mev for three solar events (ref. 28).

tive nuclear abundances in the galactic and solar cosmic rays are significantly different. The difference is primarily a result of the fact that the galactic cosmic rays have passed through several grams per square centimeter of material where fragmentation processes have increased the relative numbers of the heavier nuclei.

THE SOLAR PLASMA

In addition to the solar cosmic rays produced by large solar flares, a large number of very low energy charged particles are continuously given off by the sun. This stream of particles is often referred to as the solar wind. Gringauz, et al. (ref. 29), and Bridge, et al. (ref. 30) indicate that on quiet days during which there are no major solar flares, the velocity of the solar wind is of the order of 300 to 500 kilometers per second, with a density of about 10 protons per cubic centimeter at the orbit of the earth. It is beieved that the particle density varies with solar activity, and that the magnetic field ac-

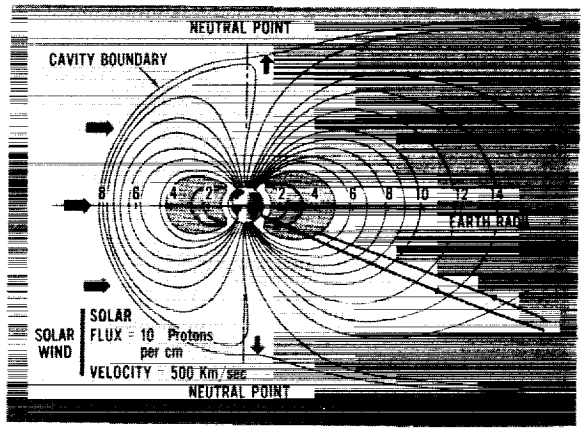

FIGURE 12–5.—The geomagnetic field and the cavity boundary configuration when acted upon by the solar wind (Ness).

companying the particles modulates the arrival of charged particles from outside the solar system as discussed earlier. Another effect of the solar plasma is to distort the shape of the geomagnetic cavity within which the earth is located. This boundary is a rather sharply defined surface separating the region within which the earth's magnetic field exerts primary control over the particle motion (the magnetosphere) from the interplanetary region. This region would be in the shape of a sphere centered at the earth in the absence of external particle motion or fields. But the solar plasma causes the magnetosphere to be compressed on the sunward side of the earth and extended away from the sun as shown in figure 12–5. The flow of the high speed plasma also creates a shock wave ahead of this magnetosphere boundary. Thus, there are three regions which must be studied, the interplanetary region, the region between the shock wave and boundary of the magnetosphere, and the magnetosphere itself. The presently available direct measurements of the quiet solar plasma have all been obtained from only three spacecraft, Lunik II, Explorer X, and Mariner II. Many of the very interesting questions about this phenomenon will have to await further data.

VAN ALLEN BELTS

The Van Allen Belt radiation consists of particles trapped in the earth's magnetosphere.

These charged particles spiral back and forth along the lines of force of the earth's magnetic field. Present evidence indicates that these particles are predominantly, and perhaps essentially exclusively, protons and electrons. The intensity and energy spectra of these particles vary greatly with the position in the trapped region and with the angle between the particle motion and the magnetic field line at any given point. Further, at least at large distances from the earth (several earth radii), rather large fluctuations of intensity with time are observed. For these reasons, a complex description of the particle properties would have to be long and detailed, and, in many respects, the picture would have to remain incomplete because of the lack of data. Therefore, only the more fundamental known characteristics will be reviewed here.

Protons

Several satellite experiments (ref. 31, 32, 33, 34, 35), including the original work of Van Allen and co-workers, have shown that the protons with energies greater than about 30 Mev are contained in a roughly doughnut-shaped region centered over the geomagnetic equator and extending from approximately 500 kilometers above the earth to about 6000 kilometers. The approximate configuration of the belt is shown in figure 12–6 (ref. 36). The maximum total intensity of protons having energies greater than 30 Mev approaches approximately 2×10^3/(cm²-sec-sr) in the heart of this region. Detailed energy spectra are available at several points in this region from the experiments of Freden and White (ref. 37, 38) and others (ref. 39) in one region, and Naugle and Kniffen (ref. 46) in another. In addition to these studies, there is additional information on the very low energy proton component. Bame, et al. (ref. 41) saw integral fluxes above 1 Mev of from 3×10^5 particles/(cm²-sec-sr) depending upon the position, but within two earth radii, and an energy spectrum from 2.7 to 7 Mev that has approximately the same slope as that observed by Naugle and Kniffen at high energies. Davis, et al. (ref. 42) see integral fluxes above 0.1 Mev. in excess of 10^6 protons/(cm²-sec-sr) at about 6 earth radii. The spectrum is again very steep and the flux is below 10^4 protons/(cm²-sec-sr) above 0.5 Mev at this large distance from the earth. These spectra are shown in figure 12–7. Finally, Freeman (ref. 43) has detected a very intense flux of particles at altitudes from 900 to 1000 Km. If these particles are assumed to be protons and reasonable assumptions are made about their energies, the results would indicate a proton flux above 0.1 Mev in excess of 10^8 protons/(cm²-sec-sr).

Electrons

Much of the existing knowledge on the electron population of the Van Allen Belts comes from the same satellite experiments referred to earlier (ref. 44). The information on the electron population is summarized in figure 12–8

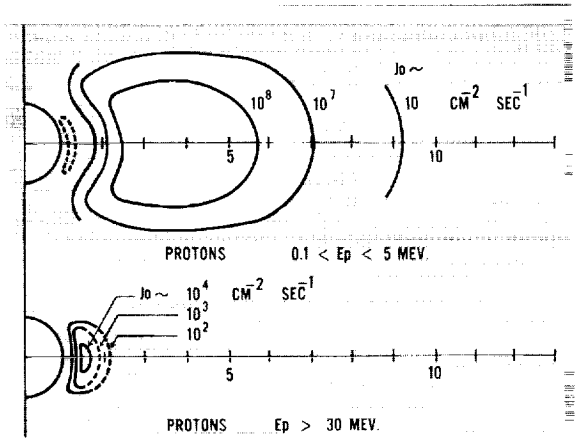

FIGURE 12–6.—Idealized diagram of the earth's proton radiation belt (Van Allen).

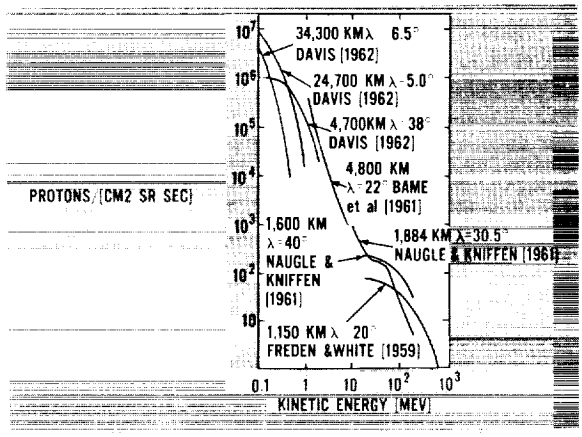

FIGURE 12–7.—Integral proton energy spectra at different points in the Van Allen belts as measured by several experimenters.

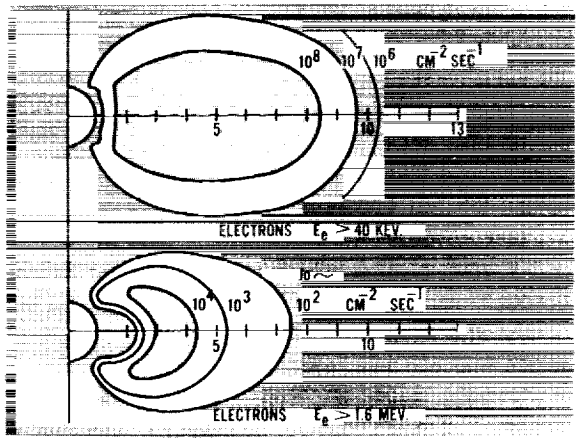

FIGURE 12-8.—Idealized diagram of the earth's electron radiation belt (Van Allen).

(ref. 36). The flux of electrons with energies greater than 1.6 Mev is known to reach a maximum at about 4 earth radii, and the electron component is observed to extend out to about 15 earth radii at the equator. There is considerable controversy over the absolute flux values and the shape of the energy spectrum, due to the difficulty of interpreting the experimental data; however, recent estimates give a flux of 5 x 10^6 electrons/(cm²-sec-sr) above 600 Kev in the region of highest intensity and 5 x 10^8 electrons/(cm²-sec-sr) above about 40 Kev.

There has been considerable speculation concerning the origin and history of the particles in the Van Allen Belts, (ref. 45) Hess, Kellog, (ref. 46), Lenchek, Singer (ref. 47), Vernov, et al. (ref. 48), and others have considered the possibility of albedo neutron decay, where the neutrons are secondaries from the interactions of galactic and solar cosmic rays in the atmosphere. There is reasonably good agreement between the flux and energy spectra of the proton component in the inner part of the belt above about 10 Mev, but there are apparently many serious disagreements, the most serious involves the flux and energy spectrum of the electrons. In order to explain the properties of the electron component, several theories related to either direct injection or local acceleration by high-frequency electromagnetic fields (ref. 46) have been suggested. However, as yet, a detailed quantitative explanation has not been obtained.

CONCLUDING REMARKS

It is clear that the field of investigation of the charged particles and magnetic fields has expanded explosively during the last five years as a result of the availability of vehicles capable of carrying detectors into space. This field of endeavor is aimed at the direct investigation of the basic questions of particle acceleration, the generation of magnetic fields in the stars, planets, and in space, and the motions of matter and magnetic fields in space. The ultimate outcome of this line of investigation should be a better understanding of a large number of broad cosmological questions, such as the development and dynamics of galaxies, the distribution of matter in the galaxies, and the physical processes occurring within and near the stars and planets.

REFERENCES

1. E. N. PARKER, Phys Rev. *109*, 1328 (1958)
2. E. FERMI, Physical Review *75*, 1169 (1949)
3. E. FERMI, Astrophysical Journal *119*, 1 (1954)
4. E. N. PARKER, Phys. Rev. Letters *107*, 830 (1957)
5. F. B. MCDONALD and W. R. WEBBER, Phys. Rev. *115* (1959) 194
6. C. FICHTEL, PhD Thesis, Washington University, St. Louis, Mo., 1959
7. C. J. WADDINGTON, Progress in Nuclear Physics *8*, Pergamon Press, 1961
8. J. EARL, Phys. Rev. Letters *6* (1961) 125
9. P. MEYER and R. VOGT. Phys. Rev. Ltrs. *6* (1961) 193
10. V. L. GINZBURG and S. I. SYROVATSKY, Prog. Theor. Phys. Suppl. *#20* (1961) 1
11. P. MEYER and R. VOGT, "Primary Cosmic Ray and Solar Protons II", submitted for publication in Physical Review
12. S. E. FORBUSH, J. Geophysical Research *59* (1954) 525.
13. S. E. FORBUSH, Terr. Magn. Atmos. Elec. *43*, 1938, 207

14. F. B. McDonald and W. R. Webber, Journal of Phys. Soc. of Japan *17*, Suppl. A–2, 1962 (428)
15. 1. Lange and S. Forbush, Terr. Magn. Atmos. Elect. *47*, 331 (1952)
16. For a summary of early work, see H. Elliott, *Progress in Cosmic Ray Physics*, North Holland Publishing Company, Amsterdam (1957)
17. G. C. Little & H. Leinback, Proc. IRE *46*, 334 (1958)
18. G. C. Reid & H. Leinback, J. Geophysical Research *64*, 1801 (1959)
19. J. R. Winckler, Journal of the Physical Society of Japan *17*, Supp. A–2, 353 (1962)
20. K. W. Ogilvie, D. A. Bryant, & L. R. Davis, J. Geophysical Research *67*, 929 (1962)
21. C. E. Fichtel and D. E. Guss, Journal of the Physical Society of Japan *17*, Supp. A–2, 321 (1962)
22. E. N. Parker, Astrophys. Jour. *133*, 1014 (1961)
23. W. R. Webber, Progress in Cosmic Ray Physics VI (1961)
24. S. Biswas, C. E. Fichtel, & D. E. Guss, to be published
25. L. R. Davis, C. E. Fichtel, D. E. Guss, and K. W. Ogilvie, Phys. Rev. Letters 6, 492 (1961)
26. D. A. Bryant, T. L. Cline, U. D. Desai, & F. B. McDonald, Bulletin of the American Physical Society II, 7, 312 (1962).
27. D. E. Guss & C. J. Waddington, Bulletin of the American Physical Society II 7, 312 (1962)
28. C. E. Fichtel, D. E. Guss, K. W. Ogilvie, Radiation Manual, to be published
29. K. I. Gringauz, V. V. Bezrukikh, V. D. Ozeroz, and R. E. Rybchinsku, Dokl. Akad. Nauk SSSR (1960)
30. H. S. Bridge, C. Dilworth, A. J. Lazarus, E. F. Lyon, B. Rossi, and F. Scherb, 1961 Proc. Kyoto IAU Conf. on Cosmic Rays and Earth Storm Kyoto, Japan, September (1961)
31. J. A. Van Allen, G. H. Ludwig, E. C. Ray, and C. E. McIlwain, IGY Satellite Series No. 3, *73* (1958)
32. J. A. Van Allen, C. E. McIlwain and G. H. Ludwig, J. Geophysical Research *64*, 271 (1959)
33. J. A. Van Allen and L. A. Frank, Nature *183*, 430 (1959)
34. S. N. Vernov, A. Y. Chudakov, P. V. Vakulov, and Y. I. Logachev, Doklady Akademii Nauk SSSR *125*, 304 (1959)
35. V. I. Krassovsky, I. S. Schlovsky, G. I. Galperin, and E. M. Svetlitsky, Proceedings of the Moskow Cosmic Ray Conference III p. 59 (1960)
36. J. A. Van Allen, private communication.
37. S. C. Freden and R. S. White, Phys. Rev. Letters *3*, 9, (1959)
38. S. C. Freden and R. S. White, J. Geophys Research *65*, 1377 (1960)
39. A. H. Armstrong, F. B. Harrison, H. H. Heckman and L. Rosen, J. Geophys. Research *66*, 351 (1961)
40. J. E. Naugle and D. A. Kniffen, Physical Review Letters 7, 3 (1961)
41. S. J. Bame, J. P. Conner, H. H. Hill, and F. E. Holly, First Western National Meeting of the American Geophysical Union, page 20, article IV (5) of the program
42. L. R. Davis, Bulletin of the American Physical Society *117*, 354
43. J. W. Freeman, "Detection of an Intense Flux of Low-Energy Protons or Ions Trapped in the Inner Radiation Zone" SUI 61–24 (1961)
44. B. J. O'Brien, J. A. Van Allen, C. D. Laughlin, and L. A. Frank, J. Geophysical Research *67*, 397 (1962)
45. W. N. Hess, Phys. Rev. Letters *4*, 11 (1959)
46. P. J. Kellog, Nature *183*, 1295 (1959)
47. S. F. Singer, Physical Rev. Letters *1*, 171 (1958)
48. Vernov and others, Fifth ESAGI Meeting, Moscow (1958)

Astronomical Research in Space

By James E. Kupperian, Jr.

DR. JAMES E. KUPPERIAN, JR., *is Head of the Astrophysics Branch of the NASA Goddard Space Flight Center. Currently he is Project Scientist for the Orbiting Astronomical Observatory. He was Project Manager and Project Scientist for the Explorer XI Gamma Ray Astronomy Satellite. Dr. Kupperian has planned and conducted research programs in the areas of solar ultraviolet photometry, upper atmosphere structure composition, auroral and airglow emissions, X-ray and Gamma Ray astronomy, satellite and rocket ultraviolet astronomy. He received his B.S. degree in Naval Architecture and Marine Engineering in 1946 from the Webb Institute, the M.S. degree in Physics in 1948 from the University of Delaware, and the Ph. D. degree in physics in 1952 from the University of North Carolina. He is a member of the American Astronomical Society, American Geophysical Union, International Astronomical Union, American Physical Society, and American Rocket Society.*

Space astronomy has opened new windows to the solar system and universe in the ultraviolet, X-ray and gamma ray spectral regions. Rewarding, if brief, observations have been made in these radiations of the sun, stars, nebulae, and the galaxy. A characteristic of these results has been their wide divergence with theoretical extrapolations of visible observations. A program of observations progressing from balloons and rockets through orbiting observatories is underway to supply the bulk of data so necessary for astronomers. These rapid strides in observing techniques presage a decade of discovery.

Of all the fields of scientific endeavor astronomy has felt the greatest impact from space flight. Studies of the earth's upper atmosphere, the moon, the planets, the sun, and interplanetary space, once the exclusive domain of the ground based astronomer, are now subject to in situ study by physicists, biologists, geologists and meteorologists. However, this recent invasion has been more than offset by the ability of space technology to remove the bounds imposed by the earth's atmosphere.

Since the turn of the century rapid strides in large telescopes, fast emulsions, and photoelectric techniques have found the astronomer approaching limits imposed by the earth's atmosphere above his telescope. Even early in this century astronomers were seeking high mountains and balloon flights in their struggle with the earth's atmosphere. With the advent of the sounding rocket and orbiting satellite, the astronomer has available a technique to eliminate the effects of the earth's atmosphere completely. Indeed, this breakthrough has been hailed by some as the greatest since the invention of the telescope.

To understand the meaning of this enthusiasm let us enumerate the limitations that the earth's atmosphere imposes upon the astronomer's observations. The atmosphere is a turbulent sea which distorts images of objects photographed or observed through it. This phenomena, which was known to the ancients as the twinkle of stars, limits optical resolution to one second of arc.

The advent of large telescopes and fast photographic emulsions has revealed another limit set by the earth's atmosphere. This limit results from the airglow layer centered about 90 km above the earth. Its diffuse light sets a background limit in the observation of faint and distant objects. Faint emissions merge into this background on long plate exposures making them undetectable.

The solar astronomer while limited by resolution is also troubled with a third problem; that of too much light. In the study of the solar corona, the solar disk is optically occulted making it possible to study the much fainter coronal emissions. The limit here is set by direct solar light scattered by the earth's atmosphere past the occulting disk of the solar coronagraph.

Finally, a most important limit set by the atmosphere is its limited transparency to electromagnetic radiation. In fact, the earth's atmosphere absorbs in more regions of the spectrum than it transmits. Most of our knowledge of the universe has been supplied by observations in visible wavelengths with small extensions into the ultraviolet and infrared regions and in the radio and microwave bands. In the infrared the constituents of the earth's atmosphere absorb in the very regions that we wish to observe the planets. Below 3000 Angstroms the earth's atmosphere is completely opaque and the far ultraviolet, the X-ray, and the gamma ray regions are accessible only using space flight techniques. The importance of this vast region is derived from the fact that the emissions and absorptions associated with the ground states of the lighter elements, the high excitation states of the heavier elements and many simple molecules plus an array of nuclear and energetic particle reactions lie in this region.

Thus, it is with the promise of escaping these bounds that we find the astronomer willing to enter the new era of space technology. It is not without problems, however, for the astronomer, traditionally a lone worker, must deal with a large engineering effort often involving thousands of engineers and technicians. He must develop remote observing techniques, and develop telescopes and detectors for use in radically different wavelength regions. Added to these management and technical difficulties,

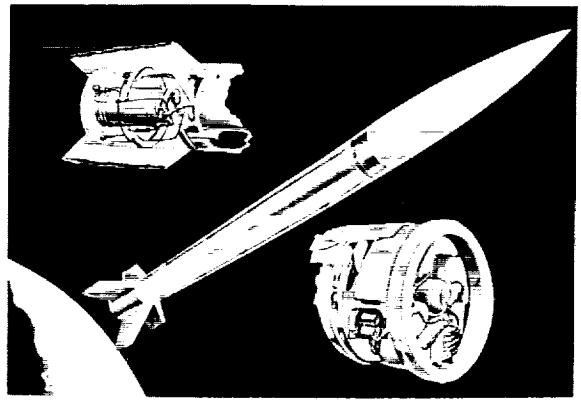

FIGURE 13-1.—The Aerobee 150A showing the location of the Attitude Control System (ACS) components. Telescopes of 12 inch aperture can be flown under a removable nosecone. Observing times above the atmosphere of 5 minutes are possible.

he must design his experimental set-up years prior to its first use with no hope of an after-the-fact adjustment that he did not design into his equipment. Despite these difficulties, the last decade has seen the orderly development of an aggressive space astronomy program. An essential element has been an ever increasing capability of rocket and satellite systems to carry the astronomer's telescopes above the atmosphere and point them at celestial objects.

Figure 13-1 shows the Aerobee rocket, the work horse of the early program and, with its recent pointing capability still the main stay of our observing program. In the early experiments, beginning in 1955, observations were obtained by small telescopes oriented to the long axis of the spin stabilized Aerobee. The spin and precessional motion of the rocket in free flight above the atmosphere scanned the telescopes across both the sky and the earth. From the optical and magnetic aspect sensors aboard the rocket, the pointing direction of each telescope for each instant of the flight was determined. This data in turn was correlated with the signals obtained from the stars and nebular objects as telemetered from the rocket. The astronomer had little or no control over what he would see, but this remains a very fruitful technique for the discovery phase of an observing program. The Aerobee has recently been supplied with an inertial attitude control system which has the capability of pointing the rocket and its payload to five preselected celes-

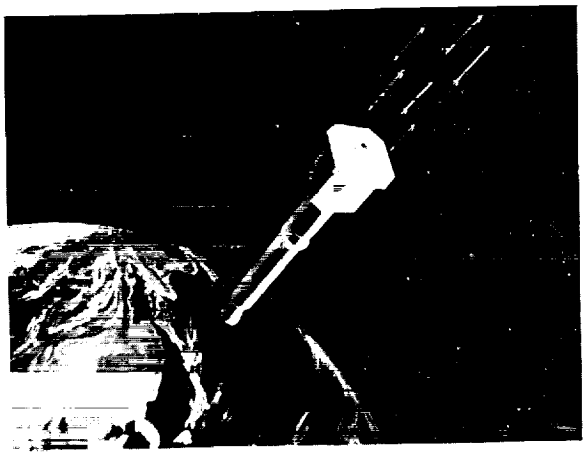

FIGURE 13-2.—Explorer XI launched April 27, 1961 showing the gamma ray telescope attached to the last stage rocket. This configuration yielded a slow scanning motion as the spacecraft progressed from a pure spinning motion to an end over end tumble.

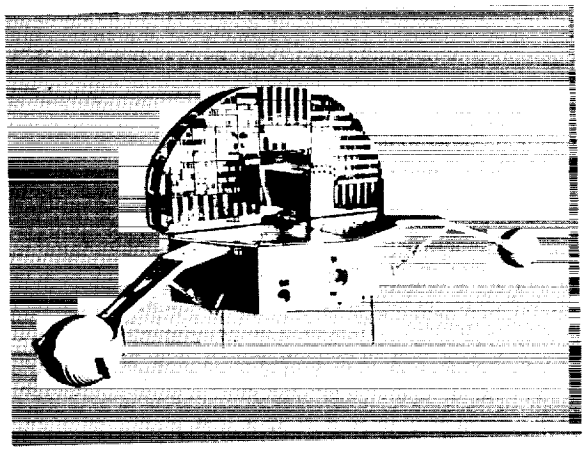

FIGURE 13-3.—The Orbiting Solar Observatory (OSO-1) launched March 7, 1962. This spacecraft pointed 75 pounds of instruments at the sun with an accuracy of 1 minute of arc. An additional 100 pounds of experiment were carried in the spinning wheel section which swept across the sun once every 2 seconds.

tial directions with an accuracy of 1½ degrees. For some applications, such as wide angle photographs or self guiding telescopes, this accuracy is sufficient. For other applications, this accurancy enables us to acquire optically the celestial objects to be studied by an error sensor. These error signals in turn actuate the servo-controls to reduce the pointing error to less than one minute of arc.

The spinning and scanning technique has been extended to satellites where more time is available to survey the sky. Explorer XI (figure 13-2) launched in April 1961 is an example of such a satellite.[1] In this case a gamma ray telescope was pointed along the long axis of the satellite. The satellite was caused to tumble end over end to scan at a slow rate. The magnetic moment of the satellite interacted with the earth's magnetic field and precessed the spin axis over the sky several times during the life of the satellite.

A more advanced observing technique combining both a scanning and pointing capability is provided by the Orbiting Solar Observatory (OSO) (figure 13-3) first flown in March of this year.[2] The OSO uses the gyroscopic properties of a spinning body for stability. The satellite has two main sections. The top part, containing two pointed experiments and a solar power supply is connected to the lower, wheel-like structure, by an axle. The pointed instruments are centered on the solar disk to within one arc minute, by counter-rotating the axle and precessing the spinning wheel with gas jets. Future versions of this system will incorporate finer pointing which will not be restricted to the center of the solar disk. The wheel of this satellite also contains experiments which scan the sky in a known fashion in relation to the sun. This payload space is useful both where it is desired to scan near the sun and where it is imperative that the experiment never sees the sun.

Finally, we consider our most difficult problem; that of pointing the telescope in orbit to an arbitrary direction on the celestial sphere. Such a device, the Orbiting Astronomical Observatory (OAO) figure 13-4, is under current development and OAO No. 1 is scheduled to be flown in 1964.[3] Up to now we have considered systems of short duration where inertial guidance is sufficient or where the observed object, i.e. the sun, can be uniquely identified. It is with the OAO that we are attempting our first celestial guidance system. The heart of the system is six small servo controlled telescopes oriented geometrically around the satellite. At all times during its orbital flight at least

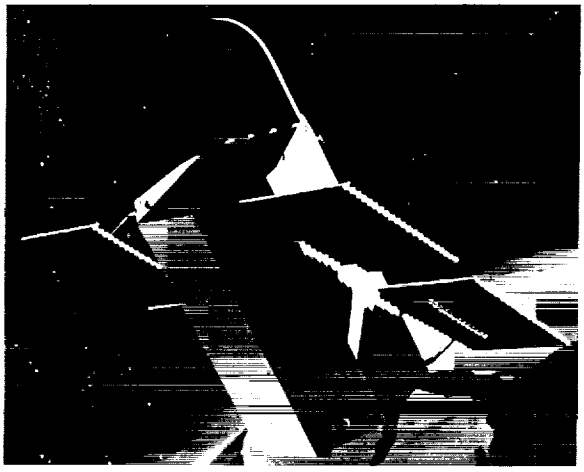

FIGURE 13–4.—The Orbiting Astronomical Observatory (OAO–1) scheduled to be launched late in 1964. Telescopes weighing up to 1000 pounds can be accommodated in a 40 inch diameter tube running the length of the spacecraft.

three of these telescopes are locked on specific stars. The switching of reference stars and the conversion of ground commands into the pointing motions of the satellite is too complicated to describe here in detail. It suffices to say that this system is designed to point the experimental telescope, to within one minute of arc, in the direction desired by the observer on the ground. At last we will have a remote observatory above the atmosphere under the control of a ground observer. The astronomer, within the limits of his telescope, will be able to modify his observing program to take advantage of current data. The one minute of arc guidance scarcely excites an astronomer but it does whet his appetite. Starting with OAO No. 2, the astronomer can feed pointing error signals generated within his telescope system to the spacecraft to increase the pointing accuracy to one second of arc. This is not the limit and, indeed, the experiment in OAO No. 3 is being designed for 0.1 second of arc guidance.

The OAO's promise to be prodigious producers of data, for here the astronomer knows no days, no cloudy nights, no light of the moon, and even no vacations.

By this time the question must arise that with all this potential is nature going to be kind and provide us with interesting data? To answer this question we go back to March 28, 1957 to an experiment done on NRL Aerobee 31.[4] This experiment utilized the scanning technique described earlier. Figure 13–5 shows the telemeter trace of one of the photometer "telescopes" flown on this flight. The "telescope" in this case was a ¼″ diameter bundle of small tubes mounted in front of a photon counter sensitive to radiation in the spectral region 1225 to 1350 Angstroms. The successive telemetering traces *a* through *d* show the signals obtained as the three degree field of view of the telescope swept the sky. The Region 1 is the constellation Orion and the Region

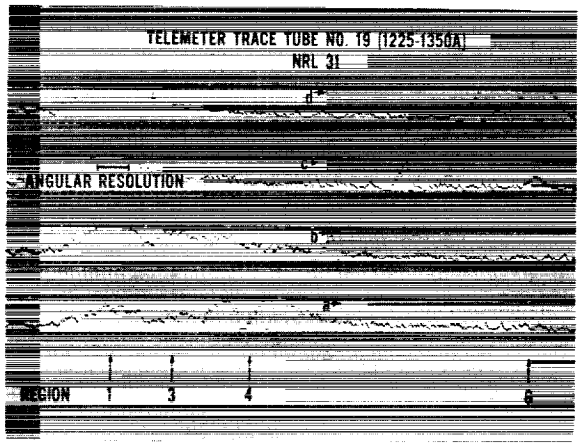

FIGURE 13–5.—Telemeter trace of a photon counter rate meter flown on March 28, 1957. Due to the precessional motion of the rocket each successive trace covers a different part of the sky. These data first revealed the extended nature of ultraviolet sources.

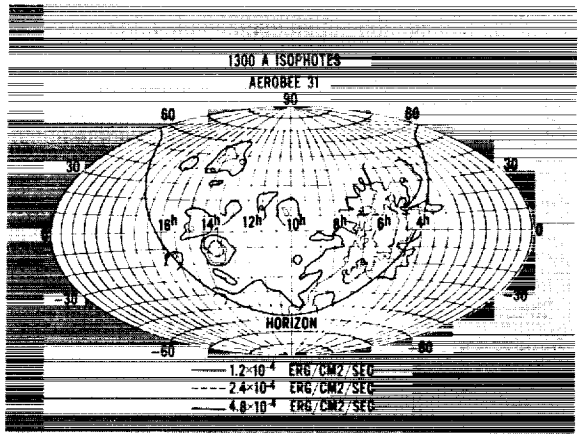

FIGURE 13–6.—Isophote map of sky at 1225–1350 A. The heavy smooth curve indicates the horizon. Trace d of Figure 5 scans from right to left about 10 degrees south of the celestial equator.

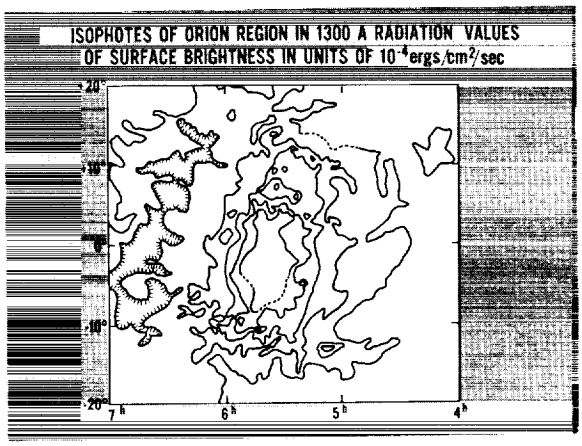

FIGURE 13–7.—Isophotes of Orion nebulosity at 1225–1350 A. Even though many early type stars were scanned in this region no point sources could be identified.

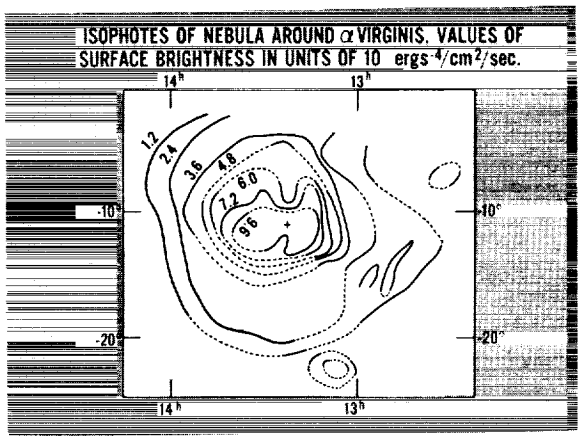

FIGURE 13–8.—Isophotes of Spica nebulosity at 1225–1350 A. The cross indicates the location of the star. This and other data reveal the nebula to emit more radiation in this wavelength region than the star.

6 is centered about the star Spica (α Virginis). These data plus that from three other telescopes has been plotted in the form of a sky map in figure 13–6. Figures 13–7 and 13–8 show the detailed isophotes of the Orion and α Virginis nebulosities. The existence of these nebulosities and in particular the one around Spica was unexpected. The fact that there is no indication of any nebulosity at visible wavelengths and that the integrated intensity of the nebula was roughly that expected from the star itself has posed a mystery that remains to this day. However, an equally significant and puzzling point was noticed in these observations. Even though Spica and a number of other stars were scanned by the detectors, no point sources were observed. Succeeding rocket observations in 1960 continued to indicate measured fluxes in the far ultraviolet approximately an order of magnitude less than predicted by theory.[5, 6] On the other hand results obtained at 2700 Angstroms by Boggess and Dunkelman[7] indicated no apparent discrepancies in other stars for longer wavelengths.

The answer to this tantalizing mystery came from an experiment by Stecher and Milligan[8] using again the scanning and precessing rocket. They devised an instrument, shown schematically in figure 13–9, to simultaneously scan the sky and record ultraviolet spectra of the stars entering the field of view of the telescope. This experiment was flown on November 22, 1960 and obtained ultraviolet spectra of 15 stars in the region 1600 to 4000 Angstroms. The telemeter traces of several of the stars observed are shown in figure 13–10. In figure 13-11 the spectra of α Carinae, a Fo star, is shown to be in good agreement with theoretical predictions. This agreement for a star not much hotter than the sun lends confidence to the remainder of the observations. Every other star observed was of earlier type and was found to be deficient in

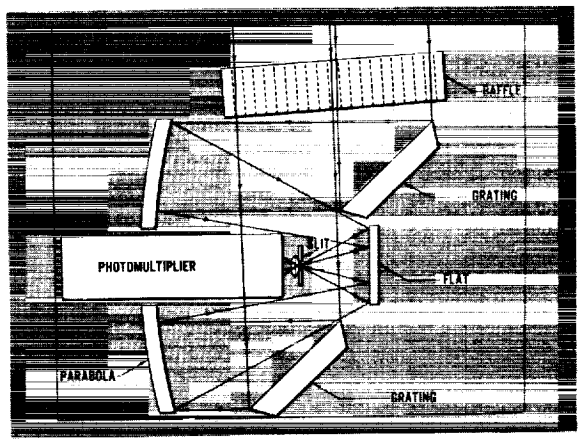

FIGURE 13–9.—Schematic of the objective grating spectrophotometer flown by T. P. Stecher and J. E. Milligan on November 22, 1960. The spin axis of the rocket is perpendicular to the plane of the drawing. Parallel stellar light enters the instrument through the baffle. The rotation of the rocket scans the spectrum across the slit. The resulting spectrum appears as a time modulated signal from the photomultiplier.

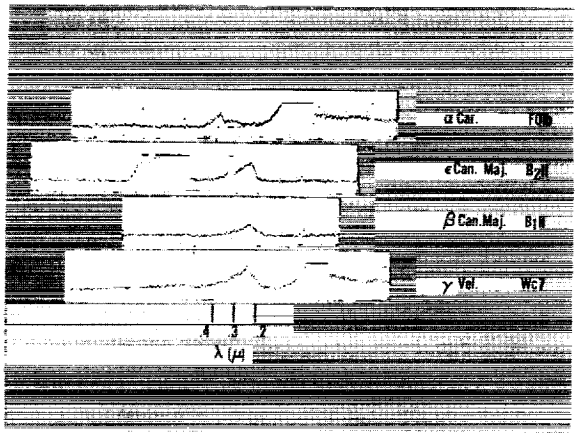

FIGURE 13–10.—Typical spectra obtained with instrument of figure 13–9.

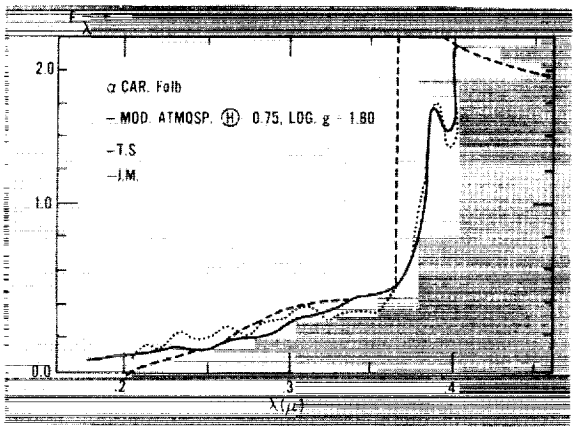

FIGURE 13–11.—The ultraviolet spectrum of α Carinae. The solid curve is the observed flux and the dashed curve is theoretical prediction.

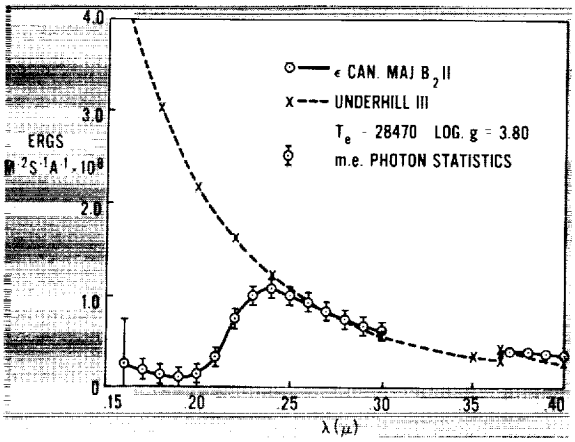

FIGURE 13–12.—The ultraviolet spectrum ε Canis Majoris. The solid curve is the observed flux and the dashed curve is theoretical prediction. The gap in the observation is due to the interference of a zero order signal of α Canis Majoris.

flux below 2400 Angstroms from that predicted from model atmospheres. The extent of the disagreement is typically illustrated in figure 13–12 by the observation and theoretical prediction for ε Canis Majoris. Stecher and Milligan conclude that this disagreement with theory can be resolved by the inclusion of an additional source of opacity due to quasi molecular absorption in the stellar atmosphere. A comparison of stars with the same classification (ε Canis Majoris, B1 II and β Canis Majoris B1 II) show spectral differences below 2400 Angstroms again emphasizing the disagreement with extrapolations from ground based data.

It should be noted that with this experiment we have tied together for the first time in a consistent picture a series of observations by different observers using different techniques of the stelar fluxes from 1225 to 3000 Angstroms. Below 2400 Angstroms and extending at least to the Lyman α line near 1216 Angstroms the fluxes of early type stars are substantially less than predicted, with the differences between stars unexplained by current stellar classifications. This is admittedly an incomplete picture lacking much in resolution and statistical coverage but it marks the beginning of an orderly observation program.

This story concerning one sequence of data can be used to stimulate a little speculation into the future. The single characteristic that stands out is that we have been surprised by every experiment that we have performed. This is due to the hazard of theoretical predictions in areas where no experimental evidence exists. It shows the beginnings of a young and promising field. Based on the one train of data, a partial list of problems to be solved emerges; the need to extend the stellar classifications to include the ultraviolet region, develop new stellar models to account for the ultraviolet deficiency, determine the reddening laws of the far ultraviolet, and assess the implications of the revised radiation field of interstellar space.

There are a number of questions still unanswered as to emission mechanisms and energy sources for ultraviolet nebulosities. These problems are as yet undetermined experimentally and more observations are needed both

in the form of surveys and observation programs devoted to specific problems.

It appears that the greatest impact on space astronomy will be its feedback to ground based astronomy and astrophysics. New detectors, remote observing techniques, and advanced electronic instrumentation will be applicable to most ground observing programs. New observations in the ultraviolet and X-ray regions in turn stimulate the need for theoretical and laboratory determinations of cross sections and F values. The need for ultraviolet and X-ray optics is stimulating research in the optical and solid state properties of materials which has already resulted in breakthroughs in optical coatings, metal mirrors, and ultraviolet photoemitters. Finally the increased emergence of astronomy in the public eye will stimulate a greater number of promising young students into considering astronomy as a career.

REFERENCES

1. KRAUSHAAR, W. L. and CLARK, G. W., Proceedings of the COSPAR Conference, Washington (1962, to be published).
2. DOLDER, F. P., BARTOE, O. E., MERCURE, R. C., JR., GABLEHOUSE, R. H., and LINDSAY, J. C., Proceedings of the COSPAR Conference, Washington (1962, to be published).
3. KUPPERIAN, J. E., JR. and ZEIMER, R. R., Inter. Science and Technology, No. 3, 48, 1962.
4. KUPPERIAN, J. E., JR., BOGGESS, A., III, and MILLIGAN, J. E., Ap. J. *128*, 453, 1958.
5. BOGGESS, A., III, "Space Astrophysics" ed. Wm. Liller, p. 121, McGraw-Hill, New York.
6. BOGGESS, A., III, Mem. Soc. R. Sc. Liege, IV 459, 1961.
7. BOGGESS, A., III, and DUNKELMAN, L., Ap. J., *129*, 236, 1959.
8. STECHER, T. P. and MILLIGAN, J. E., Ap. J. *136*, 1, 1962.

Aeronomy Research with Rockets and Satellites

By Nelson W. Spencer

NELSON W. SPENCER *is currently Head of the Physics Branch, Aeronomy and Meteorology Division of the NASA Goddard Space Flight Center. He holds a master's degree in Electrical Engineering from the University of Michigan, and is a member of the American Geophysical Union, Institute of Radio Engineers, American Rocket Society, Sigma Xi, and Eta Kappa Nu. Prior to joining the Goddard staff, Mr. Spencer was associated with the University of Michigan where he was engaged in upper atmosphere research, served as Director of the Space Physics Research Laboratory, and was a lecturer and Professor in Electrical Engineering.*

The effects of solar radiation on the earth's atmosphere are indeed profound and far reaching. Indirectly, through heating of the earth's surface and the resultant transfer of the thermal energy to the air, the lower atmosphere to altitudes of, say, 30 km is continuously agitated, circulated, and mixed. Thus the relative concentrations of the various constituents, nitrogen, oxygen, argon, carbon dioxide, and the lesser gases, are fixed. The mixing process is aided by the relatively high density of the gases because of the frequency with which the various gas particles collide and thus transfer energy, particle to particle. In the region around 50 km, ultraviolet energy is absorbed strongly by ozone, heating this region very effectively and helping to extend the mixing process to high altitudes. Figure 14–1 illustrates a typical temperature curve and indicates regions of maximum energy absorption.

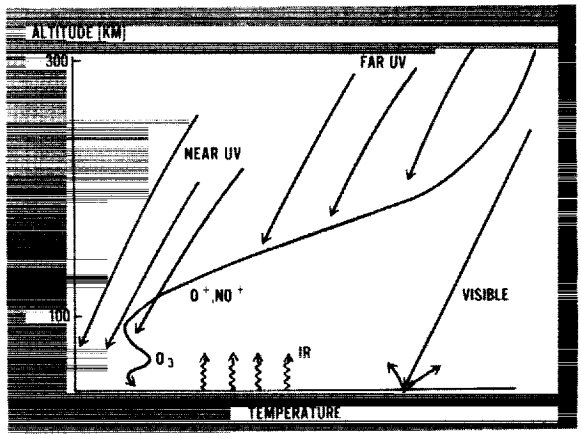

FIGURE 14–1.—Typical atmospheric temperature curve showing impinging solar radiation.

At altitudes greater than about 100 km however—and this value must be considered very approximate—the mixing process is no longer preponderant, and Dalton's law holds, increasingly with altitude. Thus, from this level upward, the various gases tend to "settle out" or "separate" according to their masses. Since the heavier gases will be concentrated at the lower altitudes, this concept of separation can be expressed in terms of the parameter: mean molecular weight. The value of this descriptive parameter in the atmosphere is thus observed to be constant at the familiar value of 28.96 up to an altitude of about 100 km, signifying fully mixed air, where it begins to decrease, reaching much lower values at greater altitudes. At the greater altitudes the lighter components helium and then hydrogen are most prominent; thus the mean molecular weight may be observed to decrease to a value of ap-

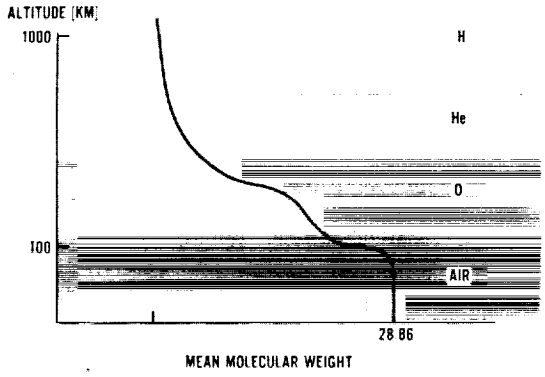

FIGURE 14–2.—Gravitational separation of atmospheric gases and mean molecular weight.

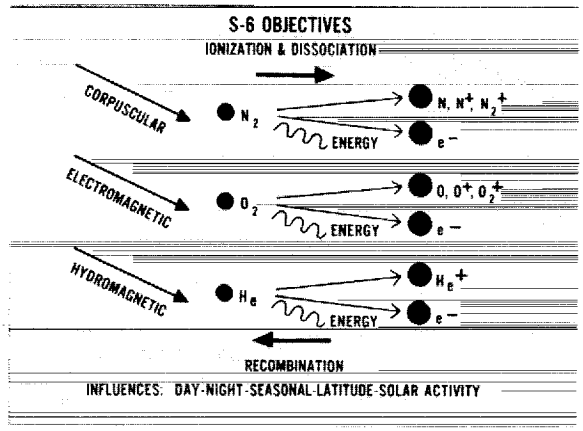

FIGURE 14–3.—Representation of atmospheric chemistry processes.

proximately 1, denoting hydrogen and ignoring the electron as a constituent. Figure 14–2 illustrates these phenomena in a conceptual manner.

Other phenomena are observed which also are of great consequence in atmospheric process considerations. Molecular gases are dissociated and ionized, and new gases are formed beginning in the 80–100 km region and above, providing an important energy sink and at the same time establishing the ionosphere.

The general atmospheric processes discussed here are characteristic of an equilibrium situation between solar infrared and other radiation absorbed directly or indirectly by the atmospheric gases, and gravitational forces acting on the atmospheric gases.

A detailed description of all atmospheric processes including dissociation, ionization, recombination, and other aspects including temperature, density, composition, and winds would be correctly described as the physics and chemistry of the atmosphere or, more appropriately, aeronomy, a name recently proposed by Professor Sidney Chapman, a renowned scientist of the upper atmosphere.

In research in aeronomy conducted to date, experimentation has been directed mostly toward a determination of (a) the composition of neutral and ion constituents, (b) temperature, (c) the density, and (d) the radiation of solar origin absorbed, reradiated, and conducted by the tenuous atmosphere. Theoretical studies have also been devoted to these aspects but in addition have emphasized energy exchange processes, the knowledge of which is fundamental to an understanding of atmospheric processes. Attention has been given to the problem of the escape of hydrogen and helium as part of the composition studies. These subjects are all interrelated; they lead to controversial theories; and they emphasize the need for better information regarding diffusion rate coefficients, cross sections, absorption coefficients, and reaction coefficients. Figure 14–3 represents the gross particle situation. Diagrammatically, processes from left to right result from solar energy input, while processes from right to left show the relaxation or recombination process that predominates when the solar input is removed.

The atmosphere, at least in its gross aspects, seems reasonably well understood above 150–200 km. Experimental data pertaining to this region have been obtained almost exclusively by studying satellite orbit decay. Results have shown strong fluctuations to be coupled with solar activity as measured, for example, by the flux of radiation in the 10 cm band.

Direct sampling of atmospheric constituents has also been accomplished through use of a few rockets and satellites. Sputnik III, the first Russian carrier for aeronomy experiments, provided crude indications of ion composition, gas density, and ion density. Explorer VIII, an American satellite provided, through ion energy measurements, a first direct indication

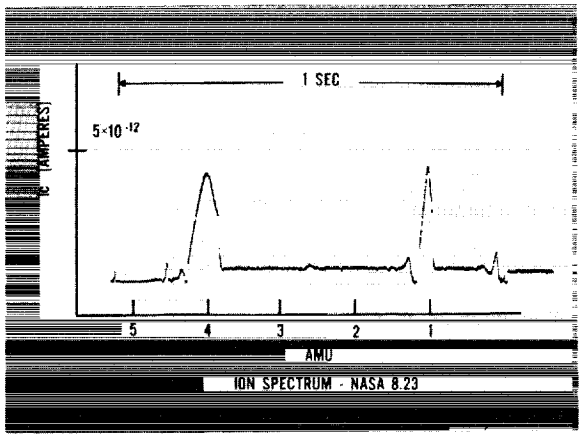

FIGURE 14–4.—Photograph of telemetry record showing direct detection of He^+ and H^+.

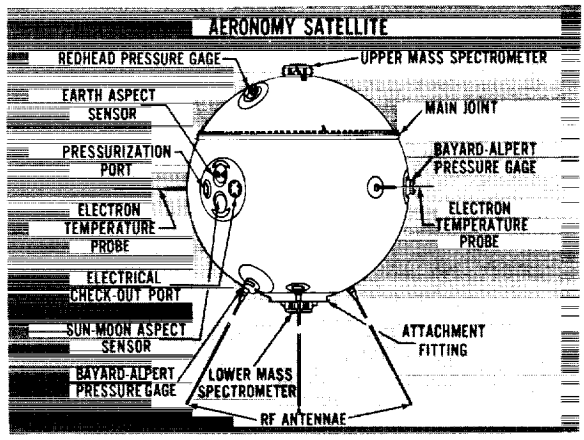

FIGURE 14–5.—Drawing of the S–6 aeronomy satellite.

of the presence of helium, making possible a correlation with similar indications from satellite drag measurements. A rocket flight accomplished about one year ago made for the first time, direct measurements and thus positive identification of helium and hydrogen ions, using an ion mass spectrometer. Figure 14–4 is a photograph of a portion of the recorded telemetry signal from this flight. The two peaks observed represent current resulting from the collection of the helium and hydrogen ions.

Measurements of the diurnal variations of neutral particle density have been made with an instrument carried by a Discoverer satellite. Indications showed a factor-of-four variation comparing density on the daytime side of the earth to the nighttime side. This confirms the fact, first detected from satellite drag measurements, that the earth's atmosphere bulges on the sunlit side as a result of atmospheric heating.

It should be noted here that all the measurements discussed have been made within about the past four years, showing that our knowledge of the aeronomy of the high altitude regions is quite recent, is certainly not far reaching, and is possibly wrong in several respects.

A new experimental attempt, on which we are working very hard, and which we hope will give us new and more precise information, involves a specialized aeronomy satellite.

It will provide for fundamental measurements of atmospheric density, temperature, pressure, composition, ion density, electron density, and electron temperature. Figure 14–5 is a line drawing of the satellite which illustrates the various components. The satellite, having a spherical shape and being vacuum tight, is designed to minimize contamination of the local atmosphere and thus permit as precise measurements by the sensors as the technology permits. This satellite will cover the altitude range of 250 to 1000 km and extend in latitude to within several degrees of the arctic and antarctic regions.

The mass spectrometer, a primary sensor system of the satellite, developed for composition measurements, is an example of the most effective means we know for determining by direct particle detection the relative concentration of helium, atomic nitrogen, atomic oxygen, molecular nitrogen, and molecular oxygen throughout the satellite's orbit.

The composition measurement problem is complex, requiring (a) that one obtain an uncontaminated atmospheric sample while the satellite is moving at a velocity of about 5 miles per second, (b) the measurement of the concentration of each constituent of the sample, and (c) the interpretation of the measurement in terms of ambient densities. Complicating factors are the large dynamic range of particle concentration the instrument must accept throughout the orbit, and the possible alteration of a sample by the presence of a hot cathode—or other metallic or catalytic surfaces that must

be there. Although this specific reference is made to problems of mass spectrometry, similar constraints are encountered in conducting any experiment that samples, in effect, the atmospheric gas. Figure 14–6 is a diagram that illustrates the basic particle movements in a magnetic spectrometer.

In addition to the aeronomy satellite the Orbiting Geophysical Observatory (OGO) series, in which several universities are already participating by conducting scientific experiments, will also provide opportunities for Aeronomy research. The EOGO (EO signifying eccentric orbit) and POGO (PO signifying polar orbit) will, in contrast to the aeronomy Satellite, cover the entire globe, extending studies into the polar regions. Figure 14–7 is a drawing of an OGO satellite.

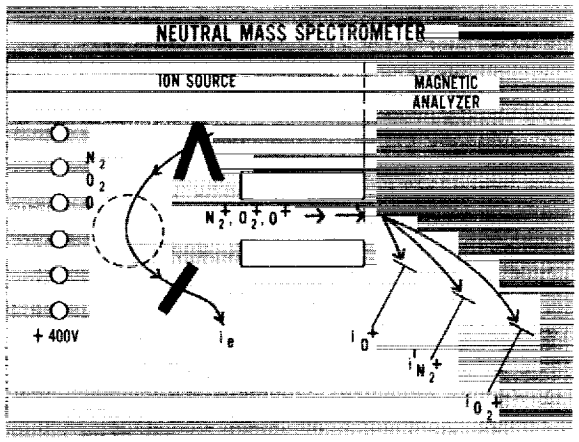

FIGURE 14–6.—Schematic diagram of particle movements in a magnetic mass spectrometer.

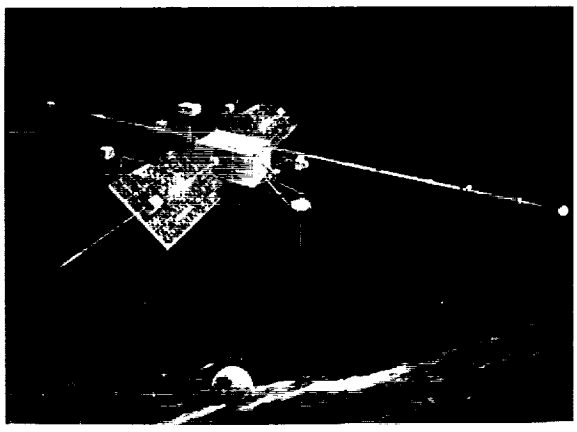

FIGURE 14–7.—OGO satellite in orbit.

All satellites, because of their high orbital velocity, enable primarily horizontally oriented investigations of an aeronomy nature. Rocket launched experiments, on the other hand, permit the experimenter to obtain a vertical profile of the atmosphere at specific locations. Several hundred launchings have been conducted during the past 16 years, many devoted to aeronomy.

Two new projects underway at the Goddard Space Flight Center provide unique examples of the kinds of aeronomy experiments now needed for continuing and productive atmospheric exploration. As in satellite experiments such as OGO where several experiments of different disciplines enabling direct correlation of results can be conducted simultaneously, the "Geoprobe" series will enable multiple experiments in aeronomy. These launchings will initially provide data to several hundred kilometers, and somewhat later to a few thousand. Measurements will include neutral particle and ion composition; neutral particle, ion, and electron density and temperature. These data will provide better insight into the separation (layering) of ions and neutral particles and will enable a better understanding of how solar ultraviolet energy is dissipated in atmospheric heating.

The Geoprobes will be concerned principally with the region above 200–300 km. For lower altitudes the TP (standing for "thermosphere probe") has been conceived. This lower altitude region is characterized by a high temperature gradient and by transition from a mixed, un-ionized atmosphere to a region of maximum charge density. Molecular oxygen is dissociated here and gaseous diffusion and conduction play controlling roles in establishing the equilibrium state. Gases can be considered singly and in hydrostatic equilibrium. The region cannot, in general, be probed by satellites; thus the geographical extent of one's knowledge is limited and will not be so easily attained. Figure 14–8 shows some characteristics of the region to be studied by the "TP." The electron temperature, believed to be particularly sensitive to solar conditions, is the parameter illustrated under differing conditions.

The experimental device being prepared will

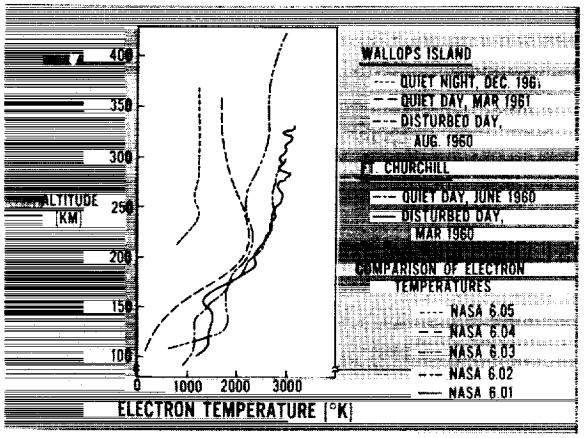

FIGURE 14–8.—Electron temperature characteristics of the ionosphere.

carry different combinations of instruments in a configuration that will be ejected from its launching rocket at about 80 km, where aerodynamic effects become insignificant in regard to the device's motion. For the first launching, the objective is to perform simultaneous independent measurements of the temperature of molecular nitrogen molecules, and electrons, in order to provide better data concerning the thermal equilibrium question. Later TP experiments will be devoted to neutral particle density and composition, and other aeronomy parameters, as have been discussed.

A review of aeronomy experiments, studies, and data interpretation problems will reveal the need for a better understanding of pertinent fundamental factors, considerations, and constants. Many of these items pose challenging problems for the critical and competent scientist. While many can be considered instrumental or technological in nature, most require, for advancement of our knowledge, recourse to very fundamental considerations of the physics and chemistry of gases and solids.

To conclude this report on aeronomy research on a note of challenge, the following listings have been drawn up to illustrate those areas where more research will permit significant fundamental advances in our understanding of planetary atmospheres. The listing is also intended to provide an indication of existing challenging topics for university scientists and students. Each item abounds in research and thesis content, and thus is suggested as one means of bringing about more extensive participation of the academic community in the nation's space exploration effort.

In specific reference to the measurement techniques, better solutions to the following problems are needed:

1. Attainment of a true ambient sample.
2. Interpretation of measured values of atmospheric samples in terms of true ambient conditions.
3. Conversion of small currents to useful signals (e.g., 10^{-27} amperes to a 5 volt signal).
4. Development of improved sensors (how one can measure pressures as low as 10^{-15} mm Hg).
5. Reliability of sensor equipment.
6. Absolute measurement of ultra-high vacuum (to 10^{-15} mm Hg or 10 particles per cm^3).
7. Generation of known and controllable beams of neutral particles (e.g., a beam of selected neutral particles of controllable velocity).

In regard to physical constants, the following are needed:

1. Better knowledge of gas reaction coefficients.
2. Better knowledge of absorption cross sections.
3. Better knowledge of gas/solid reaction coefficients.

U.S. GOVERNMENT PRINTING OFFICE : 1963 O—672058

Publ. No.	Title	Price
SP–13	Geophysics and Astronomy in Space Exploration	.35
SP–14	Lunar and Planetary Sciences in Space Exploration	.55
SP–15	Celestial Mechanics and Space Flight Analysis	.35
SP–16	Data Acquisition from Spacecraft	.40
SP–17	Control, Guidance, and Navigation of Spacecraft	.40
SP–18	Bioastronautics	.30
SP–19	Chemical Rocket Propulsion	.40
SP–20	Nuclear Rocket Propulsion	.45
SP–21	Power for Spacecraft	.25
SP–22	Electric Propulsion for Spacecraft	.35
SP–23	Aerodynamics of Space Vehicles	.40
SP–24	Gas Dynamics in Space Exploration	.40
SP–25	Plasma Physics and Magnetohydrodynamics in Space Exploration	.50
SP–26	Laboratory Techniques in Space Environment Research	.40
SP–27	Materials for Space Operations	.35
SP–28	Structures for Space Operations	.35